Dissertations, Theses, and Masters Projects   Theses, Dissertations, & Master Projects

2005

Synthesis and Characterization of Hydrogen-Rich Polyimide Materials for Radiation Shielding

Sha Yang
College of William & Mary - Arts & Sciences

Recommended Citation

SYNTHESIS AND CHARACTERIZATION OF HYDROGEN-RICH

POLYIMIDE MATERIALS FOR RADIATION SHIELDING

A Thesis

Presented to

The Faculty of the Department of Chemistry

The College of William and Mary in Virginia

In Partial Fulfillment

Of the Requirements for the Degree of

Master of Science

By

Sha Yang

2005

APPROVAL SHEET

This thesis is submitted in partial fulfillment of

The requirements for the degree of

Master of Science

SHA YANG

Sha Yang

Approved by the Committee, July 2005

Robert A. Orwoll

Robert A. Orwoll

Christopher J. Abelt

Christopher J. Abelt

Brian J. Jensen

Brian J. Jensen

TABLE OF CONTENTS

ACKNOWLEDGEMENTS

List of Tables

List of Figures

List of Schemes

ABSTRACT

In the December 9, 2003 issue of the New York Times, NASA administrator Sean O'Keefe identified radiation is "Mars mission's invisible enemy". Current radiation shielding does not provide necessary protection against high-energy cosmic radiation during outer space exploration. In this work a series of hydrogen-rich aromatic polyimides were designed because hydrogen has been found to be the most efficient atom on a weight basis for shielding against heavy ions, and benzene rings in the structure serve other ancillary functions.

Two different dianhydrides and three different diamines were used in the polymerization. Polyimide films and powders were synthesized and then characterized by inherent viscosity, elemental analysis, and thermal decomposition temperature. These aromatic polyimides can be replicated in larger quantities to produce suitable materials for radiation bombardment testing.

SYNTHESIS AND CHARACTERIZATION OF

HYDROGEN-RICH POLYIMIDE MATERIALS FOR

RADIATION SHIELDING

Chapter 1:

Introduction

Current shielding cannot provide enough protection against high-energy cosmic radiation for long-duration human space exploration. The accumulation of exposures to this radiation can significantly increase the risks of cancer to the astronauts.[1,2] The purpose of this research is to synthesize hydrogen-rich aromatic polyimides and to test their properties for radiation shielding.

The earth's magnetic field largely shields us from galactic cosmic radiation (GCR), but outside the geomagnetosphere, astronauts and equipment are endangered by full exposure to the galactic and solar cosmic ray environments. The vehicle, habitat, rover, spacesuit, and overhead atmosphere afford them only limited protection during surface operations.

In prior space missions, GCR was neglected since the mission times were relatively short. The main radiation concern were the very intense Solar Energetic Particles (SEP) events which can unexpectedly arise to dangerously high levels capable of delivering a lethal dose in a few hours.[3] Now, sufficient protection against the early effects of SEP events can be provided if the astronaut does not leave his ordinary protective quarters. In long-term deep space missions special attention is directed to GCR because the data from the Mir space station [4,5] and from space shuttle flights at high orbital inclination [6,7,8] show that more than 50% of the dose incurred by International Space Station (ISS) crew (except during solar particle events) will be from high-energy nuclei ($Z \geq 1$) in the GCR,

and of that amount a substantial fraction will be from highly charged and energetic heavy nuclei (HZE) (charge Z>2).

Serious problems are caused by GCR HZE particles because some of the particles (e.g., Fe^{+26} at 1 GeV/nucleon) [9] have enough energy to penetrate to many locations within the vehicle and habitat. The radiation exposure behind exterior walls can exceed the exposure in the absence of walls since the hull and interior materials decrease the dose per incident particle. But the colliding of HZE particles and target atoms leading to a cascade of smaller nuclei and neutrons emitted from the back side of the shield. For example, 1.3 cm aluminum shields have been typically used in spacecraft and the dose equivalent behind such shields exceeds by 10% the dose equivalent in the absence of the shield. [10]

In 1997 a NASA study group recommended the favorable shielding characteristics which include high electron density per unit mass, maximum nuclear cross section per unit mass, and high hydrogen content. [2] They provided two reasons for choosing hydrogen-rich polymers. [11] First, for charged particles, excitation and ionization of the target nuclei slow down incident particles and stop some of them. Energy loss by ionization increases with the charge-to-mass ratio of the target nucleus, Z/A (Z is atomic number and A is mass number), for a given areal density and a given incident particle. Other variables influence the ionization energy loss, but hydrogen is most effective because of its greatest stopping power per unit mass (Z/A = 1) compared to other elements (Z/A $\square$ 1/2). Second, cross sections of nuclear interactions, whereby the incident heavy ions break into lighter fragments, are approximately proportional to $(A_t^{1/3} + A_p^{1/3})^2$, where A_t and A_p are the mass numbers of target and projectile. [11] Hydrogen is

the lightest element, so hydrogen-rich shielding causes more fragmentation of the incident particle per unit mass than other sorts of shielding. Thus, by mass, hydrogen is the most efficient element for shielding against HZE particles.

In-flight measurements and accompanying model calculations[5,6,8] have shown polyethylene to be superior to aluminum for decreasing the radiation dose. [12,13] An appropriately larger thickness of the shielding will be better. In John. W. Wilson's research[14], larger shield thicknesses of 5 g/cm^2 are more effective than 1.51 g/cm^2; the latter specifications are being used in the current designs for the Mars inflatable TransHab. For larger thicknesses more energy of the projectile fragments would be absorbed and more fragments slowed down or stopped (most of the target fragments will be absorbed in the shielding material).

Radiation shielding materials should not only save weight, but also provide other ancillary functions such as structural support, insulation, plumbing, thermal conductors, and micrometeorite shields. Hydrogen-rich aromatic polyimides were synthesized in this research because polyimides are well known as high-performance polymers, which posses excellent thermal stability, inert behavior against organic solvents, and good mechanical properties. [15, 16]

CHAPTER 2:

EXPERIMENTAL

2.1. Instruction

In this work, six polyimides were synthesized by reactions of three diamines with two dianhydrides. One of the dianhydrides has a rigid structure and another one contains flexible ether ($-O-$) and isopropylidene ($-C(CH_3)_2-$) groups, which make the polyimides easy to be fabricated by increasing their solubility and moldability.[17-23] Two dianhydrides and one of the diamines are commercially available and the other two diamines were prepared.

2.2. Monomer Syntheses

2.2.1. Commercially available monomers

1,2,4,5-Benzenetetracarboxylic dianhydride (PMDA). PMDA was purchased from Aldrich and used after two sublimations (m.p. 284-286°C).
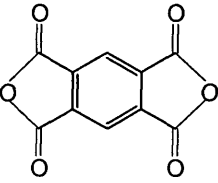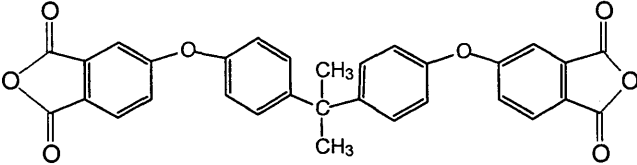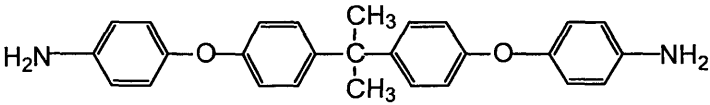
4,4′-(4,4′-Isopropylidenediphenoxy) bis (phthalic anhydride) (UDA). UDA was purchased from Aldrich and recrystallized twice from acetic anhydride to yield light brown crystals (m.p.187-188°C).[24]
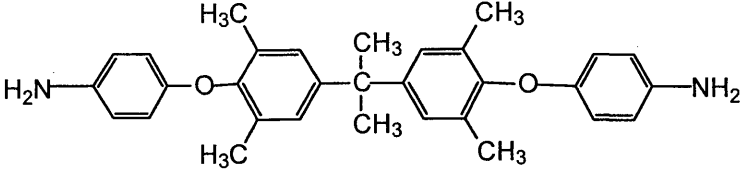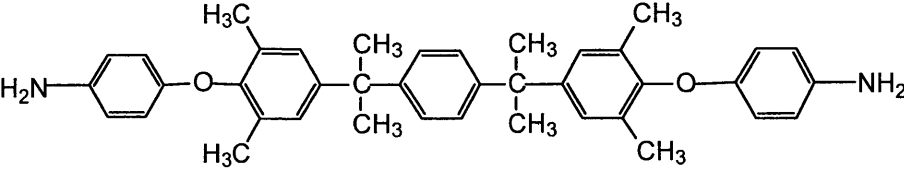
4,4′-(4,4′-Isopropylidenediphenyl-1,1′-diyldioxy)dianiline (BDA1). BDA1 was purchased from Aldrich and recrystallized twice from ethanol to yield light brown crystals (m.p. 129-130°C).

2.2.2. Monomers prepared for this study

2,2-Bis[3,5-dimethyl-4-(4-aminophenoxy)phenyl]propane (BDA2) and α,α'-bis-

[3,5-dimethyl-4-(4-aminophenoxy)phenyl]-1,4-diisopropylbenzene (BDA3) were

prepared for this research. They are listed in Table 2.1.

Table 2.1. Structure of dianhydrides and diamines

	Compound	Abbrev
Dianhy-dride		**PMDA**
		UDA
Diamine		**BDA1**

	(chemical structure)	**BDA2**
	(chemical structure)	**BDA3**

2.2.2.1. BDA2 Synthesis

2.2.2.1.1. Chemicals

2,2-bis(4-hydroxy-3,5-dimethylphenyl)propane and 4-chloronitrobenzene were purchased from TCI.

2.2.2.1.2. Synthesis of BDA2

2.2.2.1.2.1. Description of the synthesis

The synthesis of BDA2 followed D. J. Liaw's work[25], as shown in scheme 2.1. The dinitro compound was synthesized in the first step. In order to achieve a high yield, the ratio of 4-chloronitrobenzene, 2,2-bis(4-hydroxy-3,5-dimethylphenyl)-propane, and anhydrous potassium carbonate was 2.2:1:2.4. The reaction was carried out in a DMF solution with the concentration of 2,2-bis(4-hydroxy-3,5-dimethylphenyl)propane at 150-200 g/L. After refluxing in DMF overnight, the solution was cooled and poured into

a 1:1 methanol-water mixture. The crude product which precipitated was then recrystallized from glacial acetic acid.

In the second step, a reaction was carried out in an ethanol solution with the concentration of dinitro compound at 200 g/L. Hydrazine monohydrate was used as the reducing agent. The molar ratio of dinitro compound to hydrazine monohydrate was between 1:30 and1:70. The mass of the catalyst (10% Pd-C) was about 0.75%-wt of the dinitro compound. The reducing agent was drop-added when the ethanol solution started to reflux. The dinitro compound was not soluble in ethanol but the produced diamine was. So when the yellow solid (dinitro compound) disappeared in ethanol, the reaction was terminated. It took about 22 hours. The solution was then hot filtered to remove the Pd-C and was recrystallized in ethanol to yield the yellow needle-like crystal of the diamine.

Scheme 2.1: Synthesis of BDA2
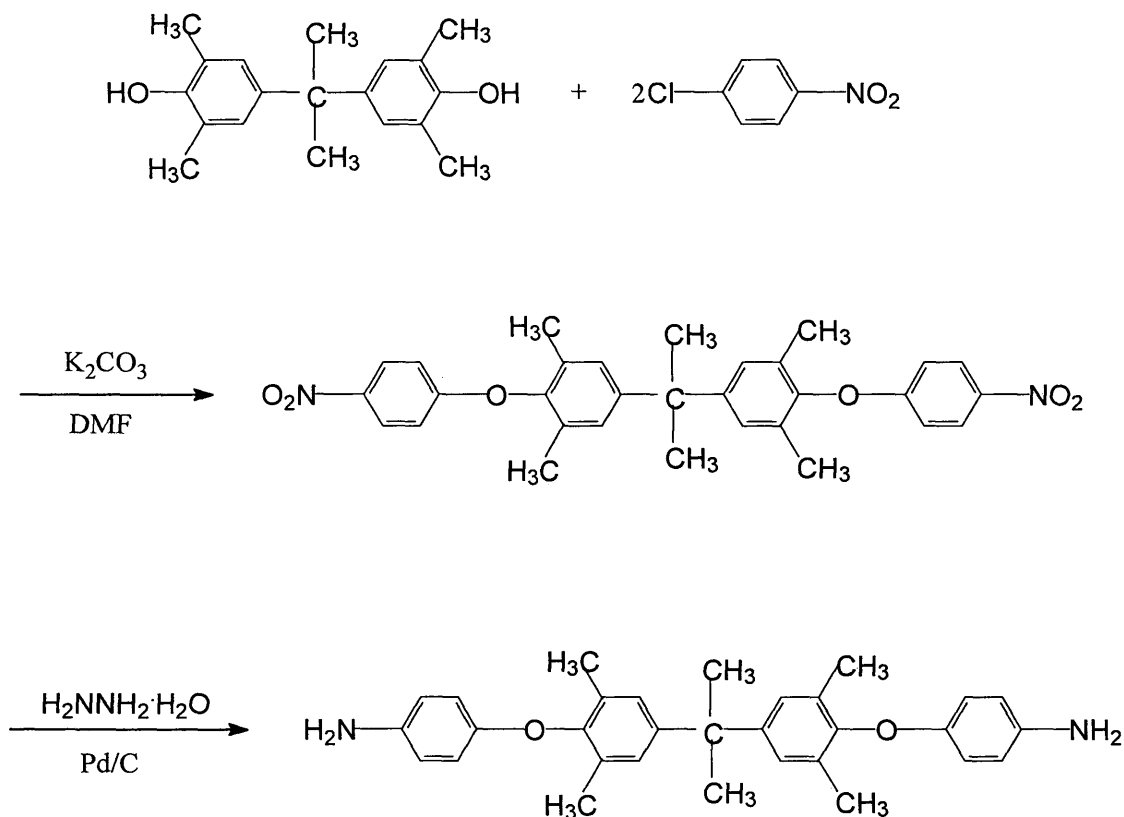
2.2.2.1.2.2. Typical synthesis

First step:

The dinitro compound was synthesized by the reaction of 2,2-bis(4-hydroxy-3,5-dimethylphenyl)propane (75.075 g, 0.26 mol) and 4-chloronitrobenzene (87.75 g, 0.56 mol) in the presence of anhydrous potassium carbonate (84.825 g, 0.62 mol) and 390 ml of DMF at 160 °C for 21 hours. The solution was then cooled down to room temperature and poured into a 1:1 methanol-water mixture. The crude product was recrystallized from glacial acetic acid to provide yellow crystals (m.p. 193-195°C) in 99.5% yield.

Second step:

138.5 g (0.26 mol) of the dinitro compound, 1.039 g of 10% Pd-C, and 693 ml ethanol were introduced into a three-necked flask to which 519 ml of hydrazine monohydrate was added dropwise at 85°C.

The reaction was continued at reflux temperature for another 22 hours. The mixture was then hot filtered to remove Pd-C. After cooling, the precipitated needle-like crystals were isolated by filtration and recrystallized from ethanol in 85.8% yield (m.p.164-166°C).

2.2.2.2. BDA3 Synthesis

2.2.2.2.1. Chemicals

α, α'-bis(4-hydroxy-3,5-dimethylphenyl)-1,4-diisopropylbenzene and 4-chloronitrobenzene were purchased from TCI.

2.2.2.2.2. Synthesis of BDA3

2.2.2.2.2.1. Description of the synthesis

A new more effective way was used to synthesize BDA3. See scheme 2.2. The yield was about 20% higher than D. J. Liaw's work[26,27,28].

The first synthetic step of BDA3 was similar to that of BDA2. The ratios of 4-chloronitrobenzene, α, α'-bis(4-hydroxy-3,5-dimethylphenyl)-1,4-diisopropyl-benzene, and anhydrous potassium carbonate were 2.2:1:2.2. The concentration of α, α'-bis(4-hydroxy-3,5-dimethylphenyl)-1,4-diisopropylbenzene was 220-250 g/L.

In the second step, hydrogenation apparatus, model 3911 from Parr, was used. Hydrogen gas was used as the reducing agent instead of hydrazine monohydrate and N,N-dimethylformamide (DMF) was used as the solvent instead of ethanol. The concentration of the dinitro compound was ca. 250 g/L of DMF. The molar ratio of dinitro compound to the consumed H_2 was about 1:6. The amount of the catalyst (10% Pd-C) was about 0.6 wt-% of the dinitro compound. The solution was stirred vigorously in room temperature. The pressure of the hydrogen gas, generally started from 50 psi, was monitored. When there was no further absorption observed, the reaction was terminated. The solution was then hot filtered to remove the Pd-C and precipitated in deionized water to yield the brown powder (diamine).

Scheme 2.2: Synthesis of BDA3
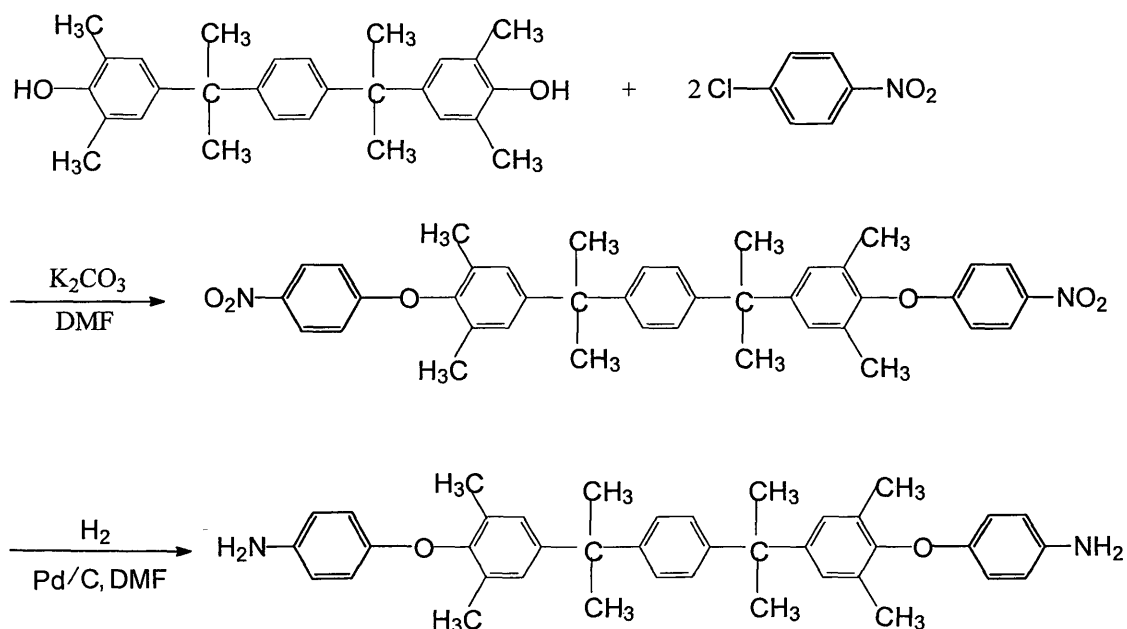
2.2.2.2.2.2. Typical synthesis

1st step:

In a flask equipped with a stirrer and a reflux condenser, there were placed 500 ml of

N, N-dimethylformamide (DMF), 120.8 g (0.3 mole) of α,

α'-bis(4-hydroxy-3,5-dimethylphenyl)-1,4-diisopropylbenzene, 104.0 g (0.66 mole) of

4-chloronitrobenzene and 91.2 g (0.66 mole) of potassium carbonate.

The resulting mixture was refluxed with stirring for 18 hours. After hot filtration, the

filtrate was cooled to precipitate α,α'-bis[3,5-dimethyl-4-(4-nitrophenoxy)phenyl]

-1,4-diisopropylbenzene (BDNPD). The mixture on the filtration paper was recrystallized

form acetic acid with the concentration of 15g/L to precipitate BDNPD.

The precipitated light yellow crystals were collected by filtration, washed with 200

ml of methanol, and dried. 168.2 g of light yellow powder was obtained. The yield was

87.0%. Melting point: 228 to 230 °C.

2nd step:

In a 500 ml reaction bottle for hydrogenator there were placed 55.0 g (0.0853 mole)

of BDNPD obtained from the preceding step, 220 ml of N,N-dimethylformamide (DMF)

and 0.33 g of a 10% Pd-C catalyst. Hydrogen gas was then introduced, while the solution

was stirred vigorously. The reaction was continued at room temperature for 72 hours. At

this point, 0.51 mol hydrogen had been absorbed. Since further absorption was not

observed, the reaction was terminated.

After completion of the reaction, the mixture was heated to 70°C to dissolve the

final product. The solid Pd-C catalyst was separated from the solution by hot filtration. The filtrate was heated to 80-90°C in an oil bath. While this temperature was maintained, 135 ml of water was added dropwise over 20 minutes in order to precipitate α,α'-bis-[3,5-dimethyl-4-(4-aminophenoxy)phenyl]-1,4-diisopropyl-benzene. The solution was slowly cooled, and the resulting light yellow crystals were collected by filtration, washed with 100 ml of methanol, and then dried. 45.9 g of α,α'-bis-[3,5-dimethyl-4-(4-aminophenoxy)phenyl]-1,4-diisopropylbenzene was collected for a yield of 91.9%. The melting point of the crystal was 226-228°C.

2.3. Polymer Syntheses

The conventional two-step polymerization method was used to prepare the polyimides, as shown in Scheme 2.3. The first step was a ring-opening polyaddition forming poly(amic acid) and the second step was thermal cyclodehydration. See Scheme 2.4 and Table 2.2.

Scheme 2.3: Procedure to make polyimide film and powder

1st step:

$$\text{Dianhydride} + \text{Diamine} \xrightarrow[\substack{\text{Overnight} \\ \text{Room Temp.}}]{\text{NMP/N}_2} \text{Poly(amic acid)}$$

2nd step:

Poly (amic acid) (PAA)

on glass → PAA film —— Cured in oven ——→ Polyimide film

in flask → PAA solution —— Heating in oil bath / Azeotrope H_2O ——→ Polyimide powder
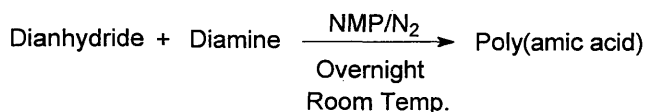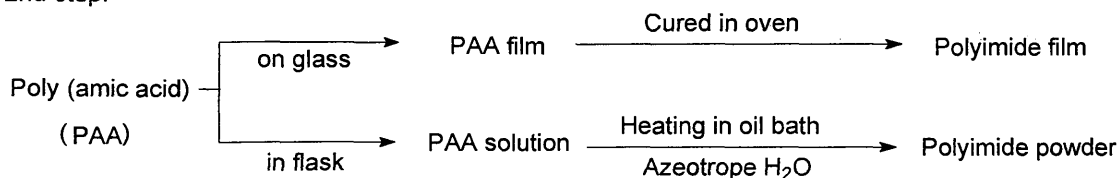
Scheme 2.4: Syntheses of polyimides
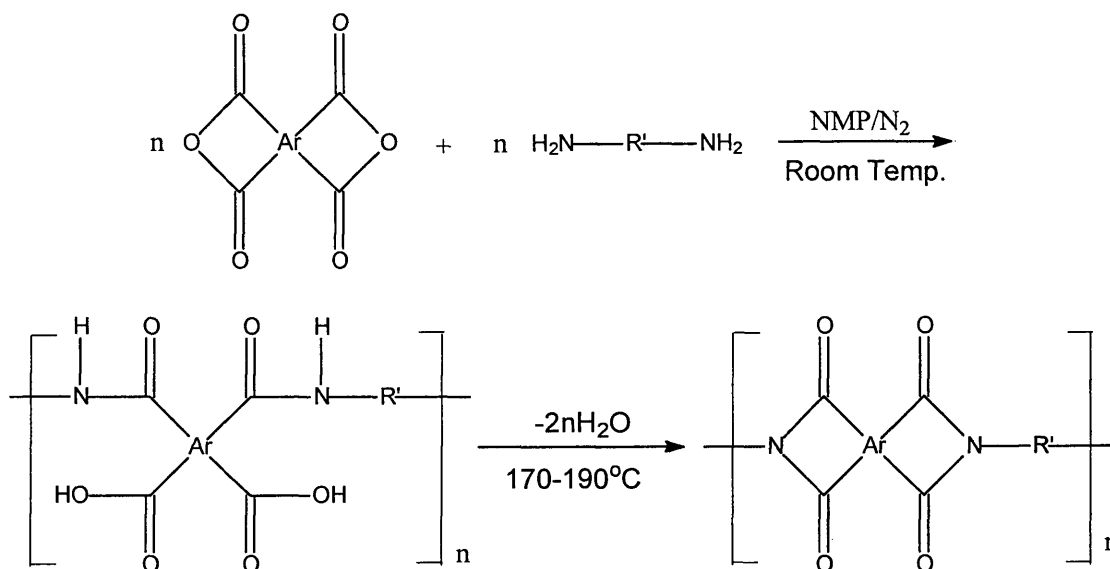
Table 2.2:Structural components in the polyimide syntheses shown in Scheme 2.4

	Compound	Abbreviation
Dianhydride cores **Ar =**		**PMDA**
		UDA
Diamine cores **R' =**		**BDA1**

	(chemical structure)	**BDA2**
	(chemical structure)	**BDA3**
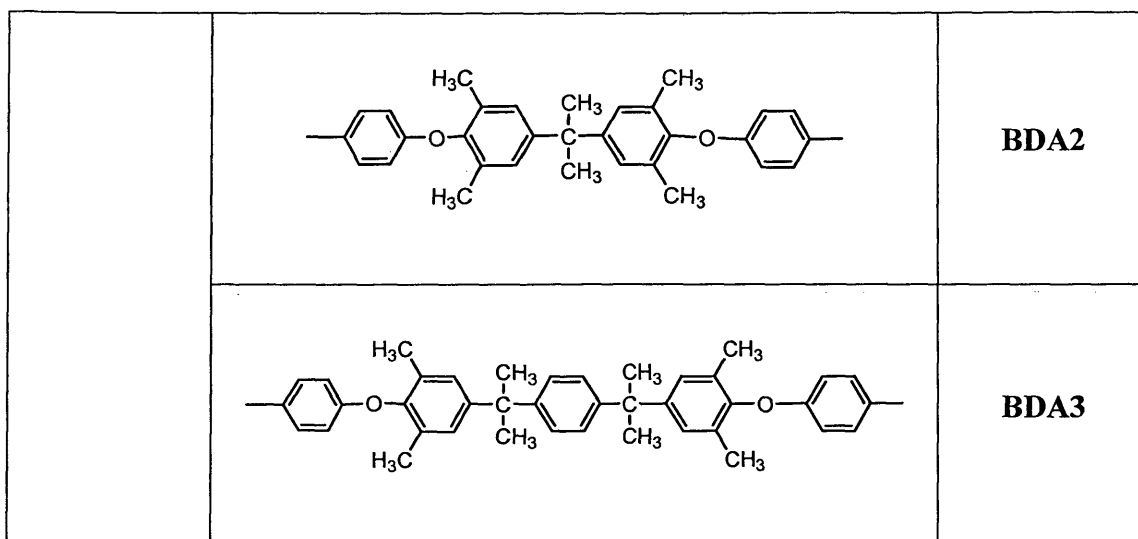
2.3.1. PMDA series

2.3.1.1. Description of the synthesis

To synthesize high molecular-weight polyimide, the mole ratio of diamine and dianhydride should be close to 1:1. The reaction mixtures were prepared with 15 wt-% solids in 1-methyl-2-pyrrolidinone (NMP).

There were two steps to make the polyimide. The first reaction which yields the poly(amic acid) should be run in the absence of air and water. This requires that the flask and the stirring blade be dried in the oven before the reaction and reaction carried out under a flow of dry nitrogen from beginning to end.

The three diamines used here dissolve in NMP, but PMDA does not. So after the diamines have dissolved in 1/3-1/2 of the total NMP needed by the reaction, PMDA was added to the solution gradually. The PMDA forms a ball in the stirred solution if it is added too fast. The first step reaction was run at room temperature overnight.

The second step is to make a polyimide film and powder. About 5 ml poly(amic acid) solution was poured onto a flat piece of clean and dry glass which had been cleaned with

ethanol and acetone, and dust was removed from the surface using a razor blade. A drawing blade was used to calibrate the solution thickness to 0.432 mm, 0.017 inches. The glass plane was kept in a low humidity chamber with dried air flowing at room temperature overnight. Then, it was put into an oven and heated to 100°C, held for one hour, heated to 200°C, held for an hour, heated to 300°C and held for one hour to make a polyimide film. To make polyimide powder, the water byproduct was removed from the imidization mixture by forming an azeotrope with toluene, which is 15 vol.% of NMP. The solution changed from transparent to opaque because the poly(amic acid) is soluble in NMP but the polyimide is not. Refluxing continued for 3-6 hours until no more water was produced. The polymer solution was then cooled and slowly poured into a blender with deionized water to precipitate the polyimide product. In the last step, hot water, then ethanol, was used to wash the polyimide powder.

2.3.1.2. Typical synthesis

27.430 g (0.126 mol) of PMDA was added gradually to a stirred solution of 73.542 g (0.126 mol) of BDA3 in 556 ml of NMP. The mixture was stirred at room temperature for 20 hours under a flow of dry nitrogen. About 5 ml of poly(amic acid) solution was used to make a film, and 84 ml of toluene was added to form an azeotrope. After refluxing for 4 hours until no more water was produced, the polyimide film and powder were made as described above. (See Scheme 2.3.) The yield was 99.5%. The syntheses of PMDABDA1 and PMDABDA2 were similar to that of PMDABDA3.

2.3.2. UDA series

2.3.2.1. Description of the synthesis

The UDA series of polyimides was synthesized in a manner very similar to that of the PMDA series. One of the differences was UDA does dissolve in NMP but PMDA does not. So in the first step, UDA and diamine were dissolved in NMP separately and the UDA solution added dropwise to diamine solution instead of adding the UDA powder to the diamine solution. Another difference was that no polyimide powder precipitated during the refluxing in the second step, because polyimides of the UDA series dissolve in NMP.

2.3.2.2. Typical synthesis

84.839 g (0.163 mol) of UDA was dissolved in 300 ml NMP and added dropwise in a stirred solution of 95.312 g (0.163 mol) of BDA3 in 692 ml of NMP. The mixture was stirred at room temperature for 20 hours under a flow of dry nitrogen. About 5 ml poly(amic acid) solution was removed from the reaction flask and used to make a film. 149 ml toluene was added to the remaining poly(amic acid) to form an azeotrope with the NMP. The polyimide film and powder were then made as described above. See Scheme 3. The yield was 99.5%. The syntheses of UDABDA1 and UDABDA2 were similar to that of UDABDA3.

2.4. Characterization methods

2.4.1. NMR

Nuclear magnetic resonance (NMR) measurements were made using a Gemini NMR 400 instrument. Samples were dissolved in $CDCl_3$ or DMSO. Both ^1H and ^{13}C resonances were studied at room temperature.

2.4.2 FTIR

FTIR measurements were made by a DIGLAB FTS 7000 IR instrument. The background of monomers was KBr and the monomers were characterized by using a KBr pellet. The polyimide films were characterized by exposure to the IR beam with a background of air.

2.4.3. Elemental analysis

The samples were tested by Atlantic Microlab.

2.4.4. Inherent viscosity

A cannon viscometer was used to test the inherent viscosity of the polymers. The inherent viscosity of a polymer solution is

$$\eta_{inh}=(1/c)\ln(\eta_p/\eta_s)\approx(1/c)\ln(t_p/t_s)$$

where c is the concentration of the polymer. 0.25 g polymer was dissolved in 50 ml NMP, so here, c is 0.5 g/dL. η_p and η_s are the viscosities of the polymer solution and of the solvent. t_p and t_s, the flow time of the polymer solution and pure solvent between the two fiducial lines on the viscometer, are taken to be proportional to their viscosities.

2.4.5. Differential scanning calorimeter measurements

Differential scanning calorimeter (DSC) measurements determined the glass transition temperatures (T_g) of the polyimides with a TA 2920 modulated differential scanning calorimeter.

In the first heating, the T_g was difficult to identify, possibly a consequence of residual solvent or incomplete imidization. In the second heating the T_g was easy to identify. Following is the detail of the procedure.

1. LNCA control: off

2. Equilibrate at 50.00 °C

3. Isothermal for 5.00 min

4. Modulate +/- 1.000 °C every 60 sec

5. Data storage: on

6. Ramp 20.00 °C/ min to 400.00 °C

7. Isothermal for 2.00 min

8. Ramp 20.00 °C/ min to 50.00 °C

9. Isothermal for 30.00 min

10. Ramp 5.00 °C/ min to 400.00 °C

11. Data storage: off

2.4.6. Thermogravimetric analyses

Thermogravimetric analyses (TGA) measurements were made using a TGA-50 thermogravimetric analyzer. Measurements were made by heating the sample from room temperature to 800°C in nitrogen atmosphere. The procedure is shown in Table 2.3.

Table 2.3: Procedure of TGA

Step	Rate of temp. increased (°C/min)	Hold temp. (°C)	Hold time (min)
1	2	110	30
2	10	600	0
3	20	800	0

Chapter 3.

Results and Discussion

3.1. Results and Discussion of monomers

3.1.1. Syntheses of monomers

Two diamine monomers BDA2 and BDA3 were synthesized on a large scale. The yields of BDA2 and BDA3 are higher than Liaw's work [25, 26, 27]. See Table 3.1. One of these two monomers, BDA3, was synthesized by using a new and more effective way. Both of the two monomers were characterized by NMR, elemental analysis, and FT-IR.

Table 3.1: Mass and yields of BDA2 and BDA3

	Dinitro Compound			Diamine Compound		
	Mass (g)		Yield (%)	Mass (g)		Yield (%)
	Single reaction	Total		Single reaction	Total	
BDA2 in Liaw's work	7.7	/	90	4	/	86
BDA2	65-146	509	95-99	46-105	324	75-86
BDA3 in Liaw's work	10	/	80	4.5	/	72
BDA3	168-194	951	87-99	38-46	570	88-96

3.1.2. Characterization of monomers

3.1.2.1. NMR

Chemical shifts of BDA2, BDA3 and the dinitro precursors for BDA2 are similar to Liaw's reports. [25, 26] [1]H shifts given above for the dinitro precursor for BDA3 were similar except for the proton ortho to the nitrogen substituent. See the NMR data in Table 3.2-3.5 and the atom number in Figure 3.1, 3.2. The spectra are Figure App. 3.7-3.14 in appendix.

Table 3.2: ^{1}H NMR Data of BDA2

	Chemical shift (ppm)		Number of atoms		Shape	
	Dinitro	Diamine	Dinitro	Diamine	Dinitro	Diamine
H_a	2.09	2.13	12	12	s	s
H_b	1.70	1.70	6	6	s	s
H_c	7.00	6.97	4	4	s	s
H_d	6.86	6.62	4	4	d	s
H_e	8.19	6.62	4	4	d	s
H_f	\	3.42	\	4	\	s

Table 3.3: ^{13}C NMR Data of BDA2

		C_1	C_2	C_3	C_4	C_5	C_6
Chemical shift (ppm)	Dinitro	16.77	31.27	42.44	142.19	126.29	130.18
	Diamine	16.97	31.37	42.21	140.21	127.41	130.70
		C_7	C_8	C_9	C_{10}	C_{11}	
Chemical shift (ppm)	Dinitro	148.21	163.03	114.99	127.80	148.17	
	Diamine	151.28	149.46	116.59	115.47	147.03	

Figure 3.1: Atom number of BDA2 and the dinitro precursor
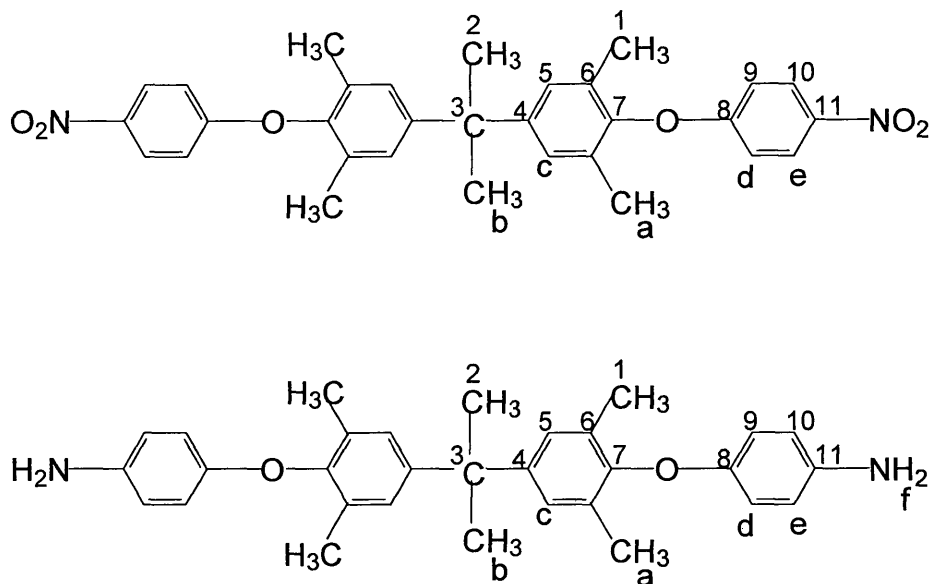
Table 3.4: ^{1}H NMR Data of BDA3

	Chemical shift (ppm)		Number of atoms		Shape	
	Dinitro	Diamine	Dinitro	Diamine	Dinitro	Diamine
H_a	2.07	1.98	12	12	s	s
H_b	1.71	1.60	12	12	s	s
H_c	7.00	6.95	4	4	s	s
H_d	6.86	6.46	4	4	d	d
H_e	8.19	6.42	4	4	d	d
H_f	7.19	7.14	4	4	s	s
H_g	/	4.66	/	4	/	s

Table 3.5: ^{13}C NMR Data of BDA3

		C_1	C_2	C_3	C_4	C_5	C_6	C_7
Chemical shift (ppm)	Dinitro	16.7	31.1	42.4	142.1	126.4	130.0	148.4
	Diamine	16.4	30.6	41.6	142.9	126.1	127.1	149.2
		C_8	C_9	C_{10}	C_{11}	C_{12}	C_{13}	
Chemical shift (ppm)	Dinitro	163.1	115.0	127.9	148.1	147.7	126.3	
	Diamine	148.6	115.1	114.7	147.3	146.2	129.9	

Figure 3.2: Atom number of BDA3 and the dinitro precursor
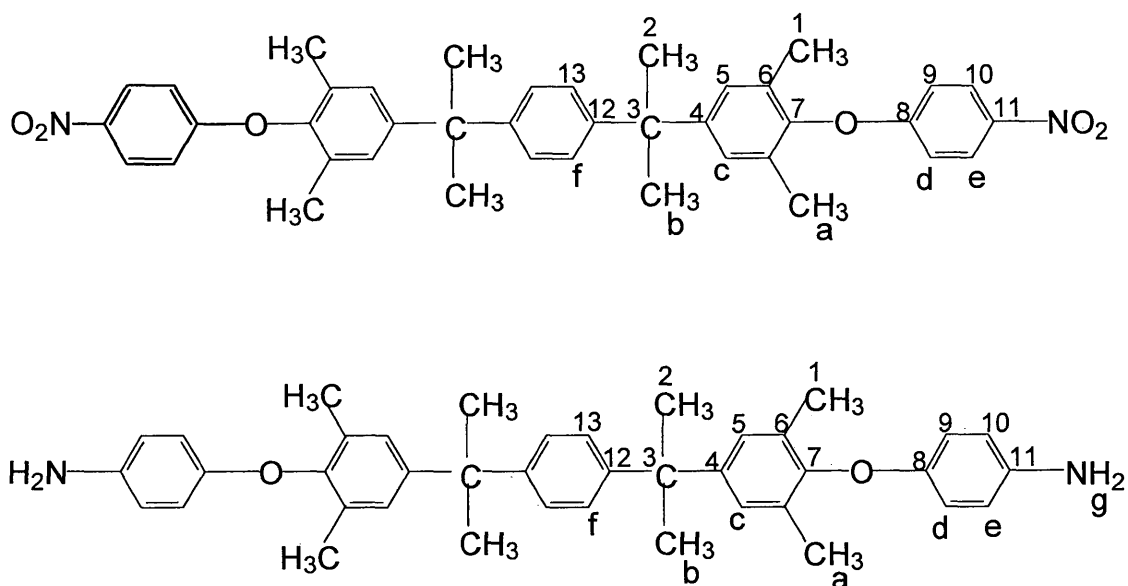
3.1.2.2. FT-IR

The infrared (FTIR) spectra of BDA2, BDA3, and their dinitio precursors are shown in Fig. 3.3-3.6. Special attention is directed to the peaks attributed to the vibrational motions of the ether linkage in the four compounds, to the N-H stretching in the two diamines, and to the vibrations of the nitro substituent in the two dinitro compounds. See Table 3.6.

Table 3.6: Significant peaks in BDA2 and BDA3

	C-O-C (cm^{-1})	N-H (cm^{-1})	NO$_2$ (cm^{-1})
BDA2 1st step product (dinitro compound)	1244	/	1588, 1346
BDA2 2nd step product (diamine compound)	1225	3407, 3366	/
BDA3 1st step product (dinitro compound)	1241	/	1594, 1339
BDA3 2nd step product (diamine compound)	1225	3440, 3360	/

Figure 3.3: FT-IR of BDA2 1st step product (dinitro compound)
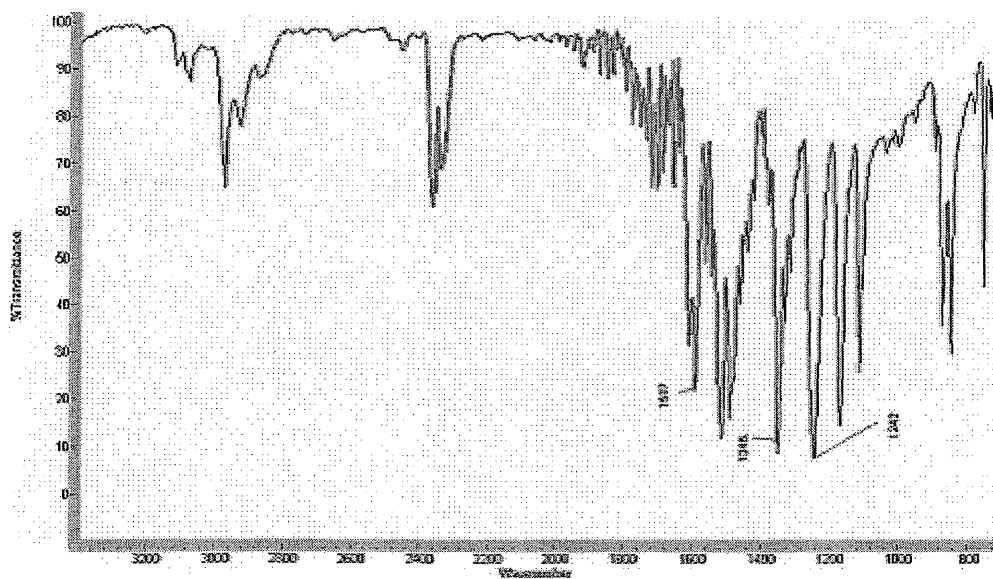
Figure 3.4: FT-IR of BDA3 1st step product (dinitro compound)
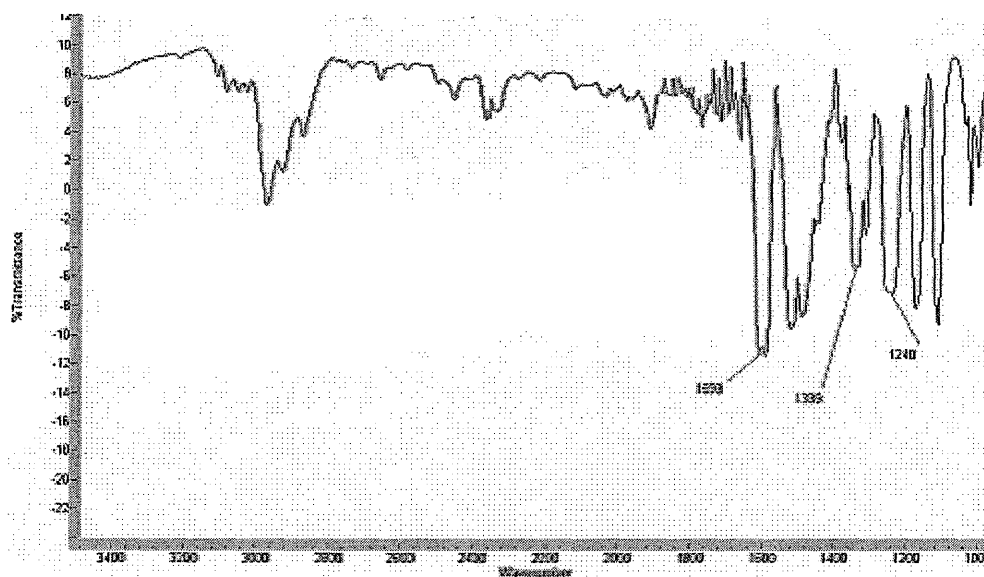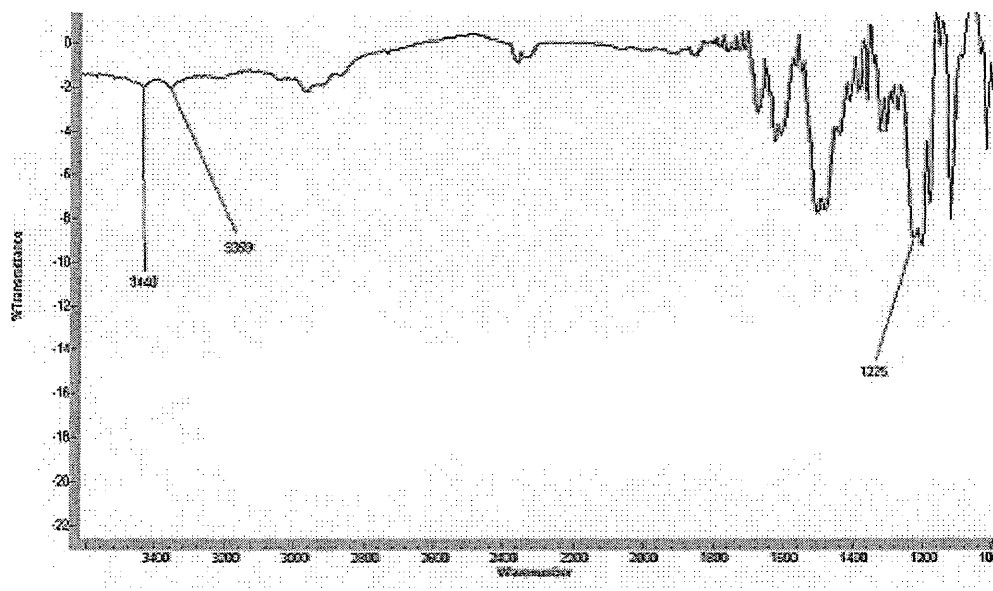

Figure 3.5: FT-IR of BDA2 2nd step product (diamine compound)

Figure 3.6: FT-IR of BDA3 2nd step product (diamine compound)

3.1.2.3. Elemental analysis

The monomers' H and N percentages were very close to the theoretical values, as shown in Table 3.7.

Table 3.7: Elemental analysis of BDA2 and BDA3

	H (%)		N (%)		C (%)	
	theory	found	*theory*	found	*theory*	found
BDA2 1st step product (dinitro compound)	*5.74*	5.75	*5.32*	5.22	*70.71*	70.23
BDA2 2nd step product (diamine compound)	*7.34*	7.30	*6.01*	6.07	*79.79*	79.38
BDA3 1st step product (dinitro compound)	*6.25*	6.19	*4.34*	4.36	*74.51*	74.38
BDA3 2nd step product (diamine compound)	*7.58*	7.65	*4.79*	5.02	*82.15*	81.23

3.2. Results and Discussion of polyimides

3.2.3. Syntheses of polyimides

Six different polyimides were prepared on a large scale at a high yield. See Table 3.8.

Both films and powders were prepared. The films were transparent, tough, and flexible.

See Figure App. 3.15 in appendix.

Table 3.8: Mass and Yields of six polyimides

Sample	Mass (g)	Yield (%)
UDABDA1	363	>95
UDABDA2	350	>95
UDABDA3	368	>95
PMDABDA1	390	92
PMDABDA2	338	>95
PMDABDA3	400	>95

3.2.4. Characterization of Polyimides

3.2.4.1. Solubilities

Several solvents were used to test the solubilities of the polyimides, as shown in Table 3.9. If at least 0.06 g of a polymer dissolved in 2 ml of the liquid at room temperature, the polyimide was judged to be "soluble". Some polyimides did not dissolve at room temperature but partially dissolved at 70°C; some others were "insoluble".

All of the polyimides were insoluble in the nonpolar solvent cyclohexane. And the UDA series of polyimides had better solubility than PMDA series. The good solubility was possibly governed by the flexible isopropylidene and arylene ether groups in the UDA unit.

Table 3.9: Solubility tests of Polyimides[*]

	cyclohexane	pyridine	DMF	DMAc	CHCl3	NMP	DMF
PMDABDA1	-	-	-	-	-	-	-
PMDABDA2	-	-	-	-	-	+ -	-
PMDABDA3	-	-	-	-	-	+ -	-
UDABDA1	-	+ +	+ +	+ +	+ +	+ +	+ +
UDABDA2	-	+ +	+ +	+ +	+ +	+ +	+ +
UDABDA3	-	+ +	+ +	+ +	+ +	+ +	+ +

*Solubility: + +, soluble at room temperature; + -, partially soluble on heating at 70°C; -, insoluble.

3.2.4.2. Inherent viscosities

The inherent viscosities of the poly(amic acid)s and polyimides are shown in Table 3.10.

Generally, high inherent viscosities correspond to high molecular weights. High molecular weight polymers generally have more desirable mechanical properties.

Table 3.10: Inherent viscosities of the poly(amic acid)s and polyimides

Sample	Viscosity of poly (amic acid) (dl/g)	Viscosity of polyimide (dl/g)
UDABDA1	0.33-0.43	0.66-0.81
UDABDA2	0.52-0.81	0.77-0.98
UDABDA3	0.23-0.39	0.21-0.54
PMDABDA1	0.53-0.57	*
PMDABDA2	0.30-0.35	*
PMDABDA3	0.36-0.48	*

*Does not dissolve in NMP.

3.2.4.3. Glass transition temperatures

Glass transition temperatures (T_g's) of polyimides, determined by means of DSC, were found to be in the range 205-234 °C for the UDA series and 291-329 °C for the PMDA series. The flexible isopropylidene and arylene ether groups in UDA contribute to their lower T_gs. See Figure App. 3.16-3.21 in appendix and table 3.11.

Table 3.11 Thermal properties of polyimides

Name	Formula	Moles of H per gram	Glass transition temperature T_g (°C) From DSC	Temp. (°C) at 5% wt. loss [a,b]	Temp. (°C) at 10% wt. loss [a,b]	Residual mass at 800°C (%)[a,c]
PMDABDA1	$C_{37}H_{24}O_6N_2$	0.041	317	473±3	498±3	49
PMDABDA2	$C_{41}H_{32}O_6N_2$	0.049	299	394±3	410±3	40
PMDABDA3	$C_{50}H_{42}O_6N_2$	0.055	281	411±7	445±6	55
UDABDA1	$C_{58}H_{42}O_8N_2$	0.047	199	436±5	499±5	55
UDABDA2	$C_{62}H_{50}O_8N_2$	0.053	233	438±5	471±5	48
UDABDA3	$C_{71}H_{60}O_8N_2$	0.056	240	463±5	476±5	48

[a] Obtained with a Shimadzu TGA-50 in flowing nitrogen (20 cm³/min) at a heating rate between ambient and 110 °C of 2 °C/min; between 110 °C and 600 °C of 10°C/min; and between 600 °C and 800 °C of 20°C/min.

[b] At least two sample tested for each polyimide.

[c] Maximum date.

3.2.4.4. Thermogravimetric analyses

The last three columns of Table 3.11 list the results of thermogravimetric analyses (TGA). All the six polyimides showed good thermal stabilities in excess of 380°C. The temperatures at 5% mass loss and 10% mass loss are 387-463 °C and 403-499 °C in nitrogen atmosphere. The residual masses at 800 °C are 40-55%.   See Figure App. 3.22-3.27 in appendix.

3.2.4.5. Elemental analysis

The polyimides' H and N percentages were very close to the theoretical values, as shown in Table 3.12.

Table 3.12: Elemental analysis[*] of polyimides

	H (%)		N (%)		C (%)	
	theory	found	*theory*	found	*theory*	found
PMDABDA1	*4.08*	3.97	*4.73*	4.55	*75.00*	74.45
PMDABDA2	*4.97*	5.03	*4.32*	4.32	*75.91*	75.34
PMDABDA3	*5.52*	5.51	*3.65*	3.76	*78.31*	77.01
UDABDA1	*4.73*	4.84	*3.13*	3.08	*77.84*	77.45
UDABDA2	*5.30*	5.34	*2.95*	2.97	*78.30*	78.02
UDABDA3	*5.66*	5.64	*2.62*	2.66	*79.75*	79.71

[*]Tested by Atlantic Microlab.

3.2.4.6. FT-IR

Bands close to 1777 cm^{-1}, 1712 cm^{-1}, and 1375 cm^{-1} were found in the FT-IR spectra of the six polyimides films. These three bands can be attributed to the asymmetric and symmetric stretches of the carbonyl group and C-N stretching respectively. See Figure App. 3.28-3.33.

3.3. Conclusions

Two diamines and six polyimides were successfully prepared in high purity, high yield and large quantity in this study. Three of the polyimides have excellent solubility and all the six polyimides showed good thermal stabilities in excess of 380°C. The polyimide films are transparent and flexible and may have good tensile properties.

Chapter 4:

Summary and Conclusions

In this research (1) a more effective way was used to synthesize diamines on a large scale so that the yield and quantity of the monomers are higher than those in Liaw's work; (2) six polyimides were successfully prepared on a large scale (about 338-400 g of the polyimide powder for each of the six kinds of polyimides); and (3) several polyimide blocks (See Figure App. 4.1 and Table App. 4.1 in appendix) were made to test their properties as shields against high-energy cosmic radiation.

The polyimide materials studied in this research are expected to be able to serve useful functions in addition to the shielding, which are not served by commercially available polyethylene, because the polyimides have aromatic units in the backbone for favorable mechanical, thermal and outgassing properties and (2) have higher densities of hydrogen atoms than highly aromatic, high-performance polymers such as Kapton.

More characterization, including mechanical testing, is planned for these materials. The radiation testing of the materials listed in Table 3.11 and Table App. 4.2 (in appendix) at the NASA Space Radiation Laboratory (NSRL), as well as the calculations predicting the properties of these materials as shielding, is in progress.

References

1. National Council on Radiation Protection and Measurements: Guidance on radiations received in space activities. (1989), NCRP Rep. No. 98.

2. J. W. Wilson, J. Miller, A. Konradi, F. A. Cucinotta, Eds., *Shielding Strategies for Human Space Exploration*, (1997), NASA C.P. 3360.

3. J. W. Wilson, F. M. Denn. Preliminary analysis of the implications of natural radiations on geostationary operations. (1976), NASA TN D-8290.

4. G. D. Badhwar, A. Konradi, W. Atwell, M. J. Golightly, F. A. Cucinotta, J. W. Wilson, V. M. Petrov, I. V. Tchernykh, V. A. Shurshakov and A. P. Lobakov. Measurements of the linear energy transfer spectra on the Mir orbital station and comparison with radiation transport models. *Radiat. Meas.* (1996), 26, 147-158.

5. F. A. Cucinotta, J. W. Wilson, J. R. Williams and J. F. Dicelllo. Analysis of Mir-18 results for physical and biological dosimetry: radiation shielding effectiveness in LEO. *Radiat. Meas.* (2000), 32, 181-191.

6. G. D. Badhwar and F. A. Cucinotta. Depth dependence of absorbed dose, dose equivalent and linear energy transfer spectra of galactic and trapped particles in polyethylene and comparisons of calculations with models. *Radiat. Res.* (1998),149, 209-218.

7. T. Sakaguchi, T. Doke, N. Hasebe, T. Hayashi, T. Kashiwagi, J. Kikuchi, S. Kono, S. Nagaoka, T. Nakano and S. Takahashi. LET distribution measurement with a new real-time radiation monitoring device-III onboard the space Shuttle STS-84. *Nucl. Instrum. Methods Phys. Res.* (1999), *A* 437, 75-87.

8. G. D. Badhwar and F. A. Cucianotta. A comparison of depth dependence of dose and linear energy transfer spectra in aluminum and polyethylene. Radiat. Res. (2000),153, 1-8.

9. J. A. Simpson. *Composition and Origin of Cosmic Rays* (M. M. Shapiro, Ed.), (1983), p. 1. Reidel, Dordrecht.

10. M. Y. Kim, J. Wilson, S. A. Thibeault, J. E. Nealy, F. F. Badavik, and R. L. Kiefer, Performance Study of Galactic Cosmic Ray Shield Materials, (1994),NASA TP-3473.

11. J. Miller, C. Zeitlin, F. A. Cucinotta, L. Heilbronn, D. Stephens and J. W. Wilson.. Benchmark Studies of the Effectiveness of Structural and Internal Materials as Radiation Shielding for the International Space Station. *Radiation Research*(2003), 159, 381-390.

12. J. W. Wilson, M. Kim, W. Schimmerling, F. F. Badavi, S. A. Thibeault, F. A. Cucinotta, J. L. Shinn and R. Kiefer, Issues in space radiation protection: Galactic cosmic rays. *Health Phys.* (1995), 68, 50-58.

13. J. R. Letaw, R. Silberberg and C. H. Tsao, Radiation hazards on space missions outside the magnetosphere. *Adv. Space Res.* (1989), 9, 285-291.

14. Lisa C. Simonsen, John. W. Wilson, Myung H. Kim, and Francis A. Cucinotta.. Radiation exposure for human Mars exploration. *Health Physics Society* (2000), 79 (5), 515-525.

15. D. Wilson, H. D. Stenzenberger; P. M. Hergenrother, Eds., *Polyimides*, Chapman and Hall, New York 1990.

16. M. I. Bessonov, M. M. Koton, V. V. Kudryavtsev, L. A. Laius, Eds., *Polyimides*, Consultants Bureau, New York 1987.

17. Critchley, J. P.; White, Mary A.. Perfluoroalkylene-linked aromatic polyimides. II.Further property studies. *Journal of Polymer Science, Polymer Chemistry Edition* (1972), 10(6), 1809-25.

18. Arnold, C. A.; Summers, J. D.; McGrath, J. E.. Synthesis and physical behavior of siloxane modified polyimides. *Polymer Engineering and Science* (1989), 29(20), 1413-18.

19. Tsutsumi, Naoto; Tsuji, Akiyoshi; Horie, Chika; Kiyotsukuri, Tsuyoshi. Preparation and properties of silicon-containing polyimides. *European Polymer Journal* (1988), 24(9), 837-41.

20. Beltz, Mark W.; Harris, Frank W.. Synthesis and properties of aromatic polyimides containing oxyalkylene linkages. *High Performance Polymers* (1995), 7(1), 23-40.

21. Tjugito, Sukanto; Feld, William A.. Polyimides derived from 1,2-bis(4-aminophenoxy)propane. *Journal of Polymer Science, Part A: Polymer Chemistry* (1989), 27(3), 963-70.

22. Charbonneau, L. F.. Synthesis and properties of alkylene-linked aromatic polyimides. *Journal of Polymer Science, Polymer Chemistry Edition* (1978), 16(1), 197-212.

23. Liaw, Der-Jang; Yang, Wen-Chung Ou; Li, Lain-Jong; Yang, Mei-Hui. Synthesis

and properties of novel aromatic polyimides derived from bis(p-aminopheoxy)methylphenylsilane. *Journal of Applied Polymer Science* (1997), 63(3), 369-376.

24. Sachindrapal, P.; Nanjan, M. J.; Shanmuganathan, S. Synthesis of aromatic polyimides containing ether linkage. *Makromolekulare Chemie, Rapid Communications* (1980), 1(11), 667-70.

25. Liaw, D.; Liaw, B. Synthesis and characterization of new soluble polyimides derived from 2, 2-bis[3,5-dimethyl-4-(4-aminophenoxy)phenyl]propane. *Macromol. Chem. Phys.* (1998), 199, 1473-1478.

26. Liaw, D.; Liaw, B.; Yu. C. Synthesis and characterization of new organosoluble polyimides based on flexible diamine. *Polymer* (2001), 42, 5275-5179.

27. Liaw, D.; Huang, H. P.; Hsu, P. N.; Chen, W. H. Synthesis and Characterization of New Highly Soluble Polyamides Derived form α, α'-Bis[3,5-dimethyl-4-(4-aminophenoxy)phenyl]-1,4-Diisopropylbenzene. *Polymer Journal* (2002), 34(5), 307-312.

28. Hu, Y.; Yang, S.; Park, C. S.; Orwoll, R. A.; Jensen, B. J. (2004).*Polymer Preprints.*45(2), 673-674.

Appendices
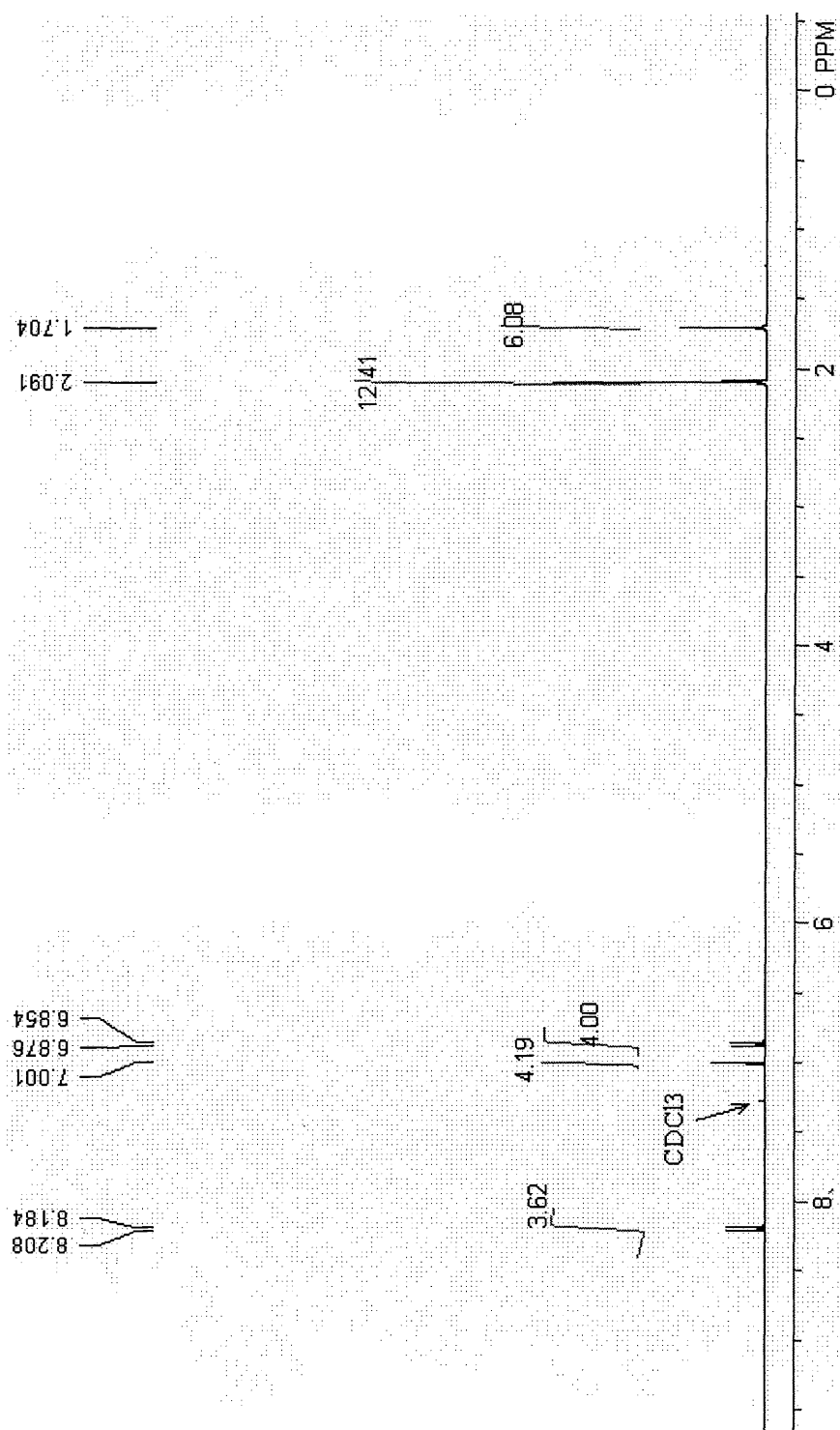
Figure App. 3.7: ^{1}H NMR of BDA2 dinitro compound
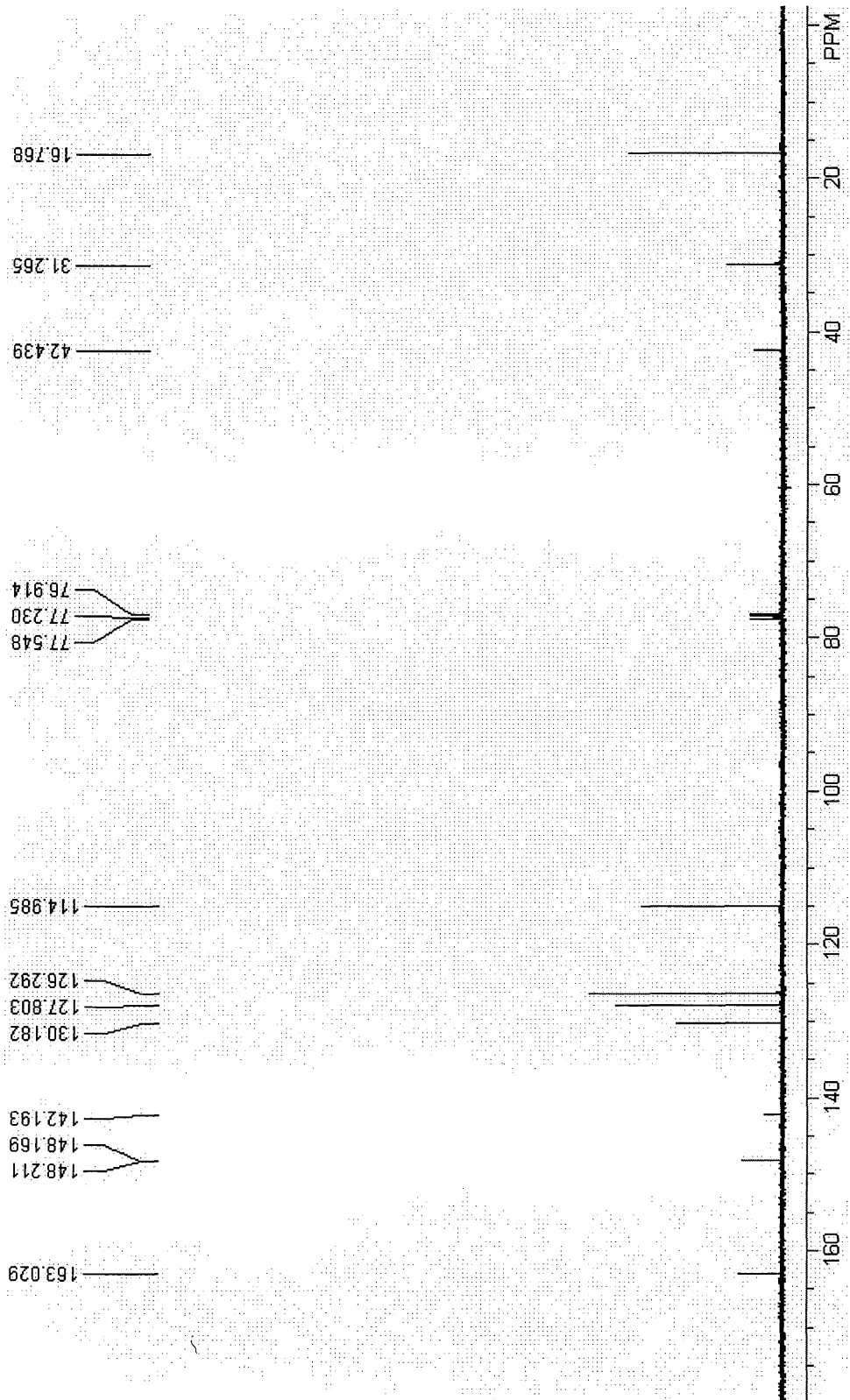
Figure App. 3.8: ^{13}C NMR of BDA2 dinitro compound
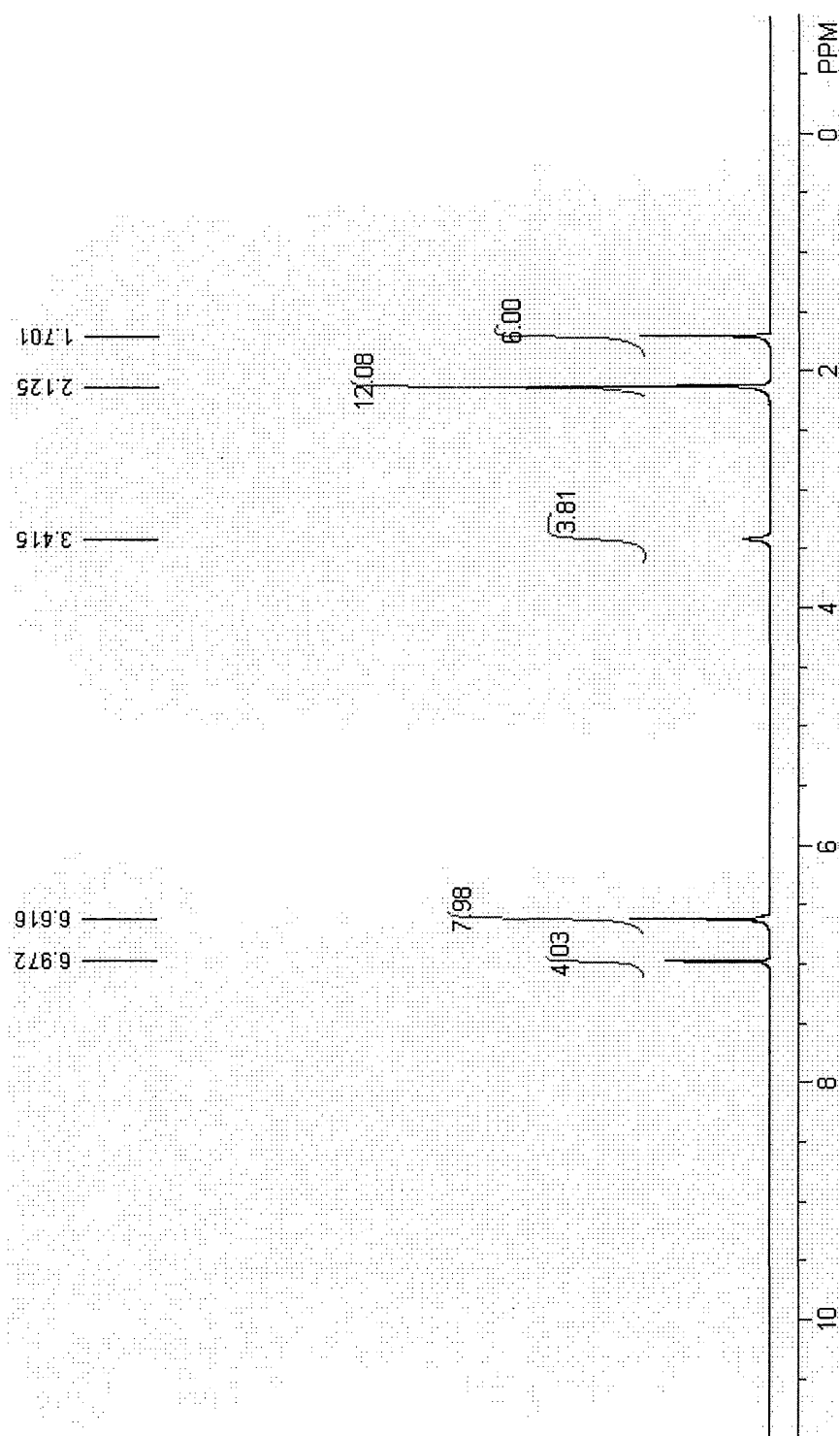
Figure App. 3.9: ^{1}H NMR of BDA2

16.974

31.372

42.208

76.915
77.230
77.554

115.474
116.594

127.408
130.698

140.213

147.029
149.458
151.277

PPM

20

40

60

80

100

120

140

160
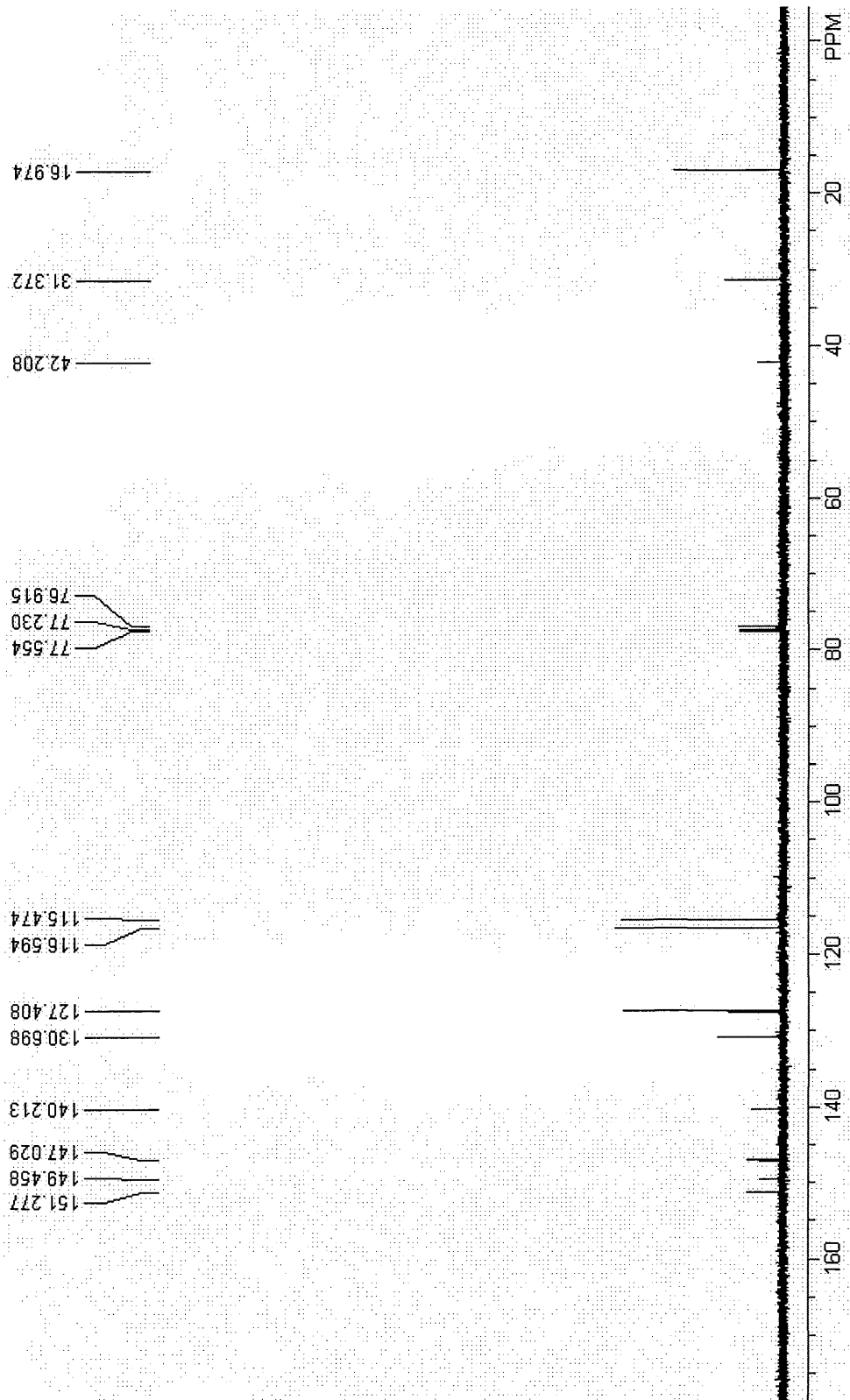
Figure App. 3.10: ^{13}C NMR of BDA2
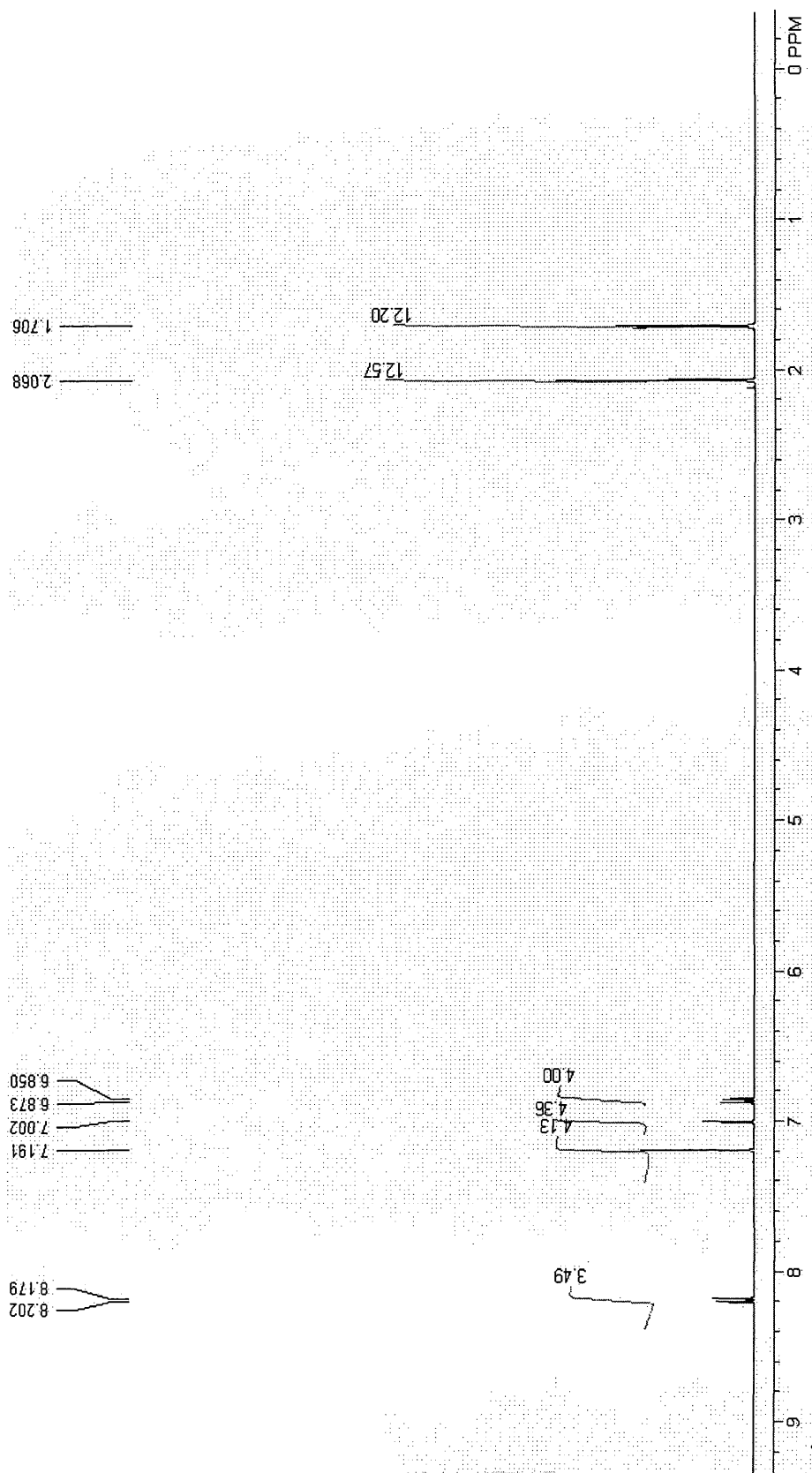
Figure App. 3.11: ^{1}H NMR of BDA3 dinitro compound

16.710

31.141

42.410

76.907
77.230
77.547

114.979

126.276
126.442
127.912
129.991

142.149
147.673
148.107
148.447

163.058

PPM

20

40

60

80

100

120

140

160
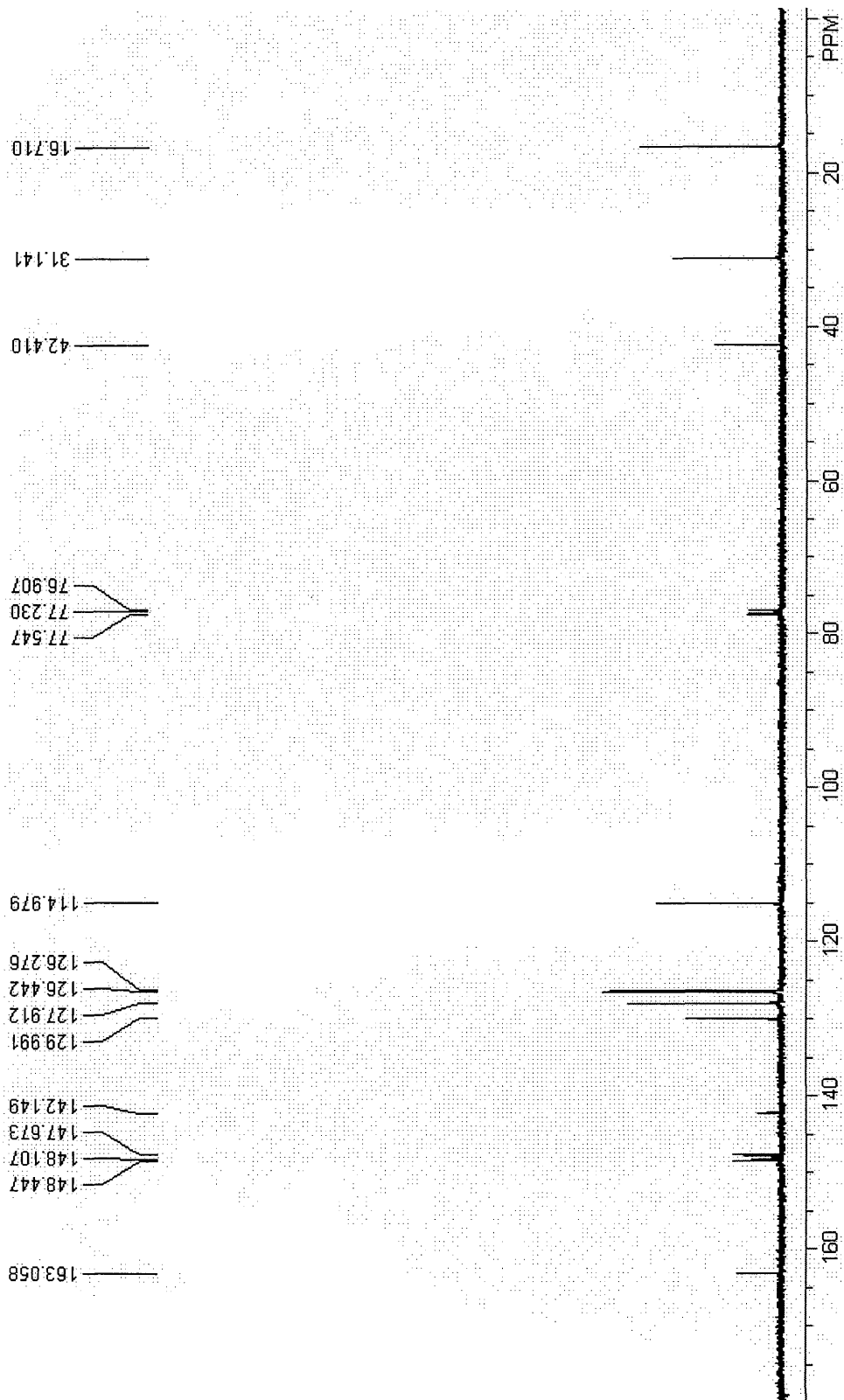
Figure App. 3.12: ^{13}C NMR of BDA3 dinitro compound
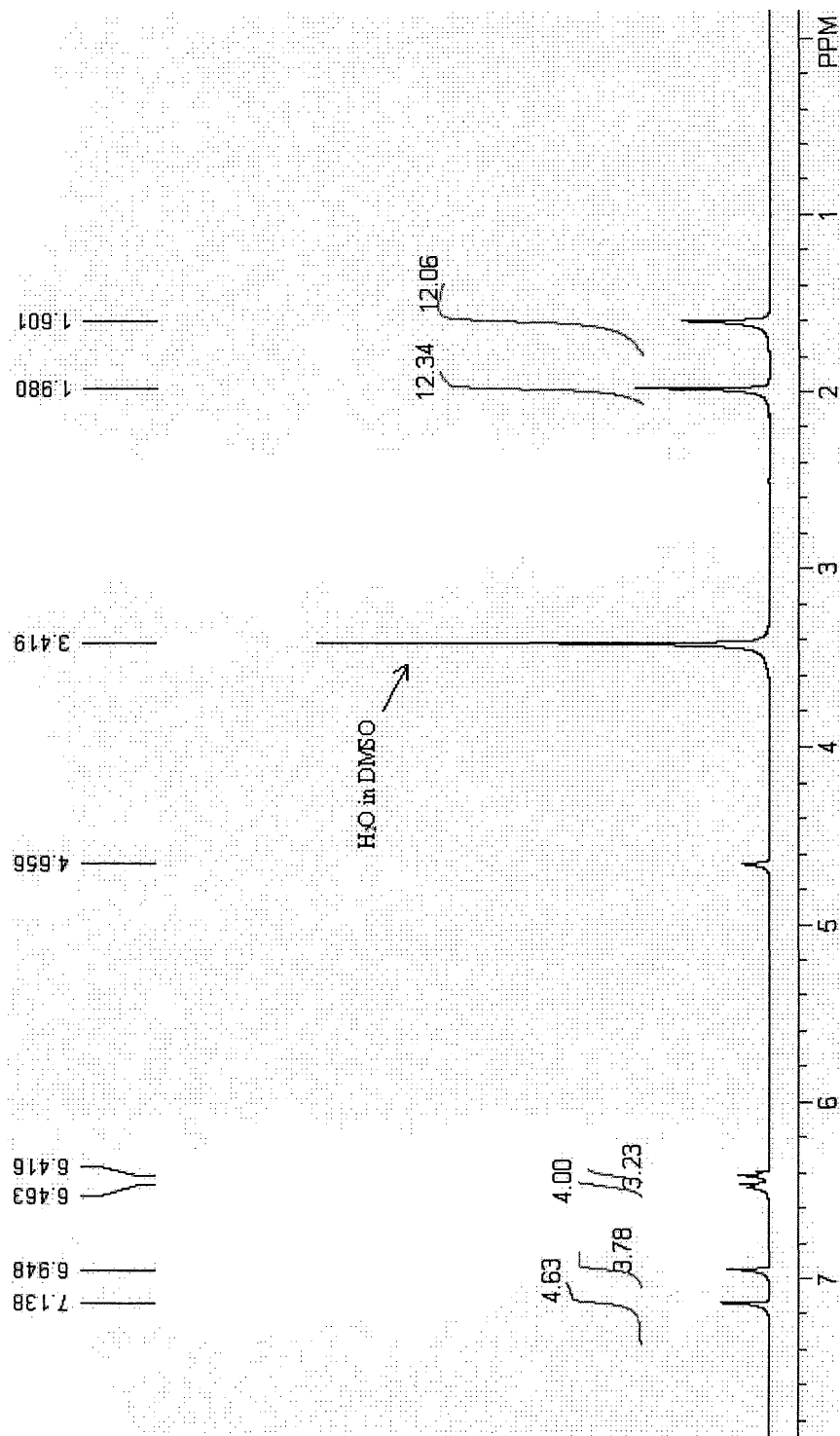
Figure App. 3.13: ^{1}H NMR of BDA3

16.438
30.600
38.888
39.093
39.302
39.510
39.717
39.925
40.133
41.600

114.716
115.095
126.054
127.057
129.933
142.869
146.196
147.348
148.607
149.166

DMSO

PPM
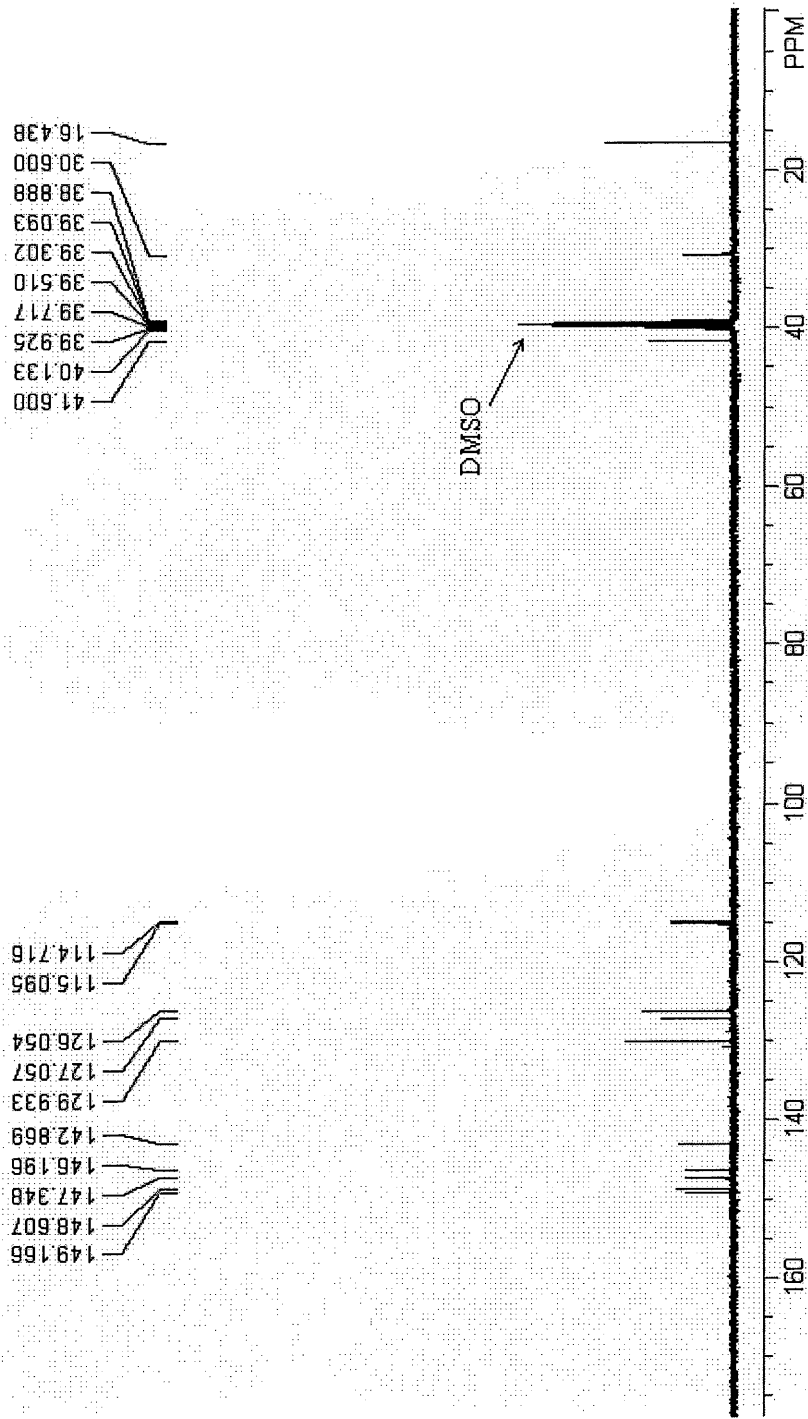
Figure App. 3.14: ^{13}C NMR of BDA3

PMDABDAI

UDABDAI

PMDABDA2

UDABDA2

PMDABDA3

UDABDA3

Figure App. 3.15: Six polyimide films

DSC

306.32°C

317.42°C(I)

325.33°C

Temperature (°C)

Rev Heat Flow (W/g)

Exo Up

Universal V3.0G TA Instruments

Figure App. 3.16: DSC of PMDABDA1

DSC

Sample: PMDA-BDA2 film 080204
Size: 8.7000 mg
Method: Cell Constant

File: C:\ahuy\pmda-bda2-022805_1.001
Operator: Judd
Run Date: 28-Feb-05 11:56

286.82°C

298.92°C(I)

314.97°C

Universal V3.0G TA Instruments

Temperature (°C)

Rev Heat Flow (W/g)

Exo Up
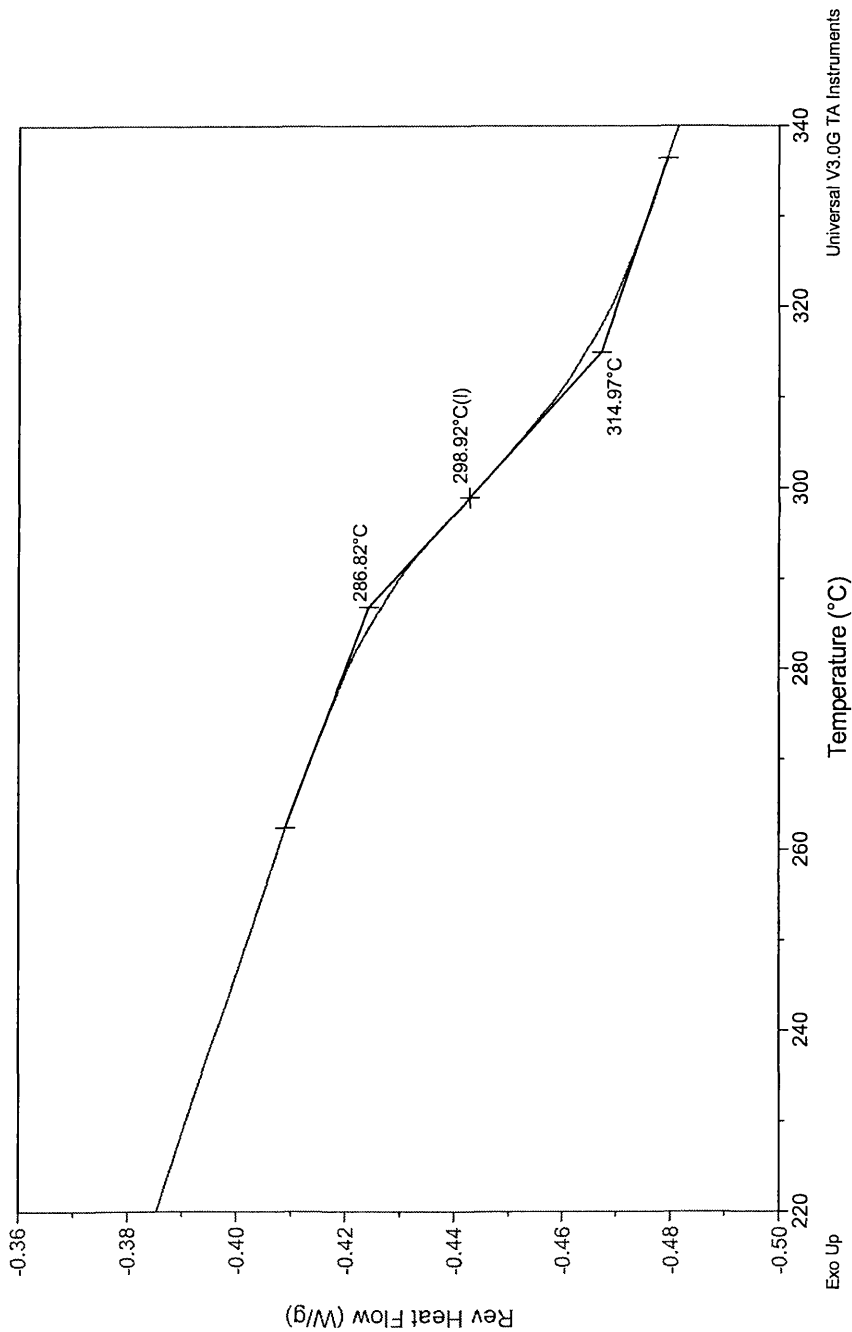
Figure App. 3.17: DSC of PMDABDA2

DSC
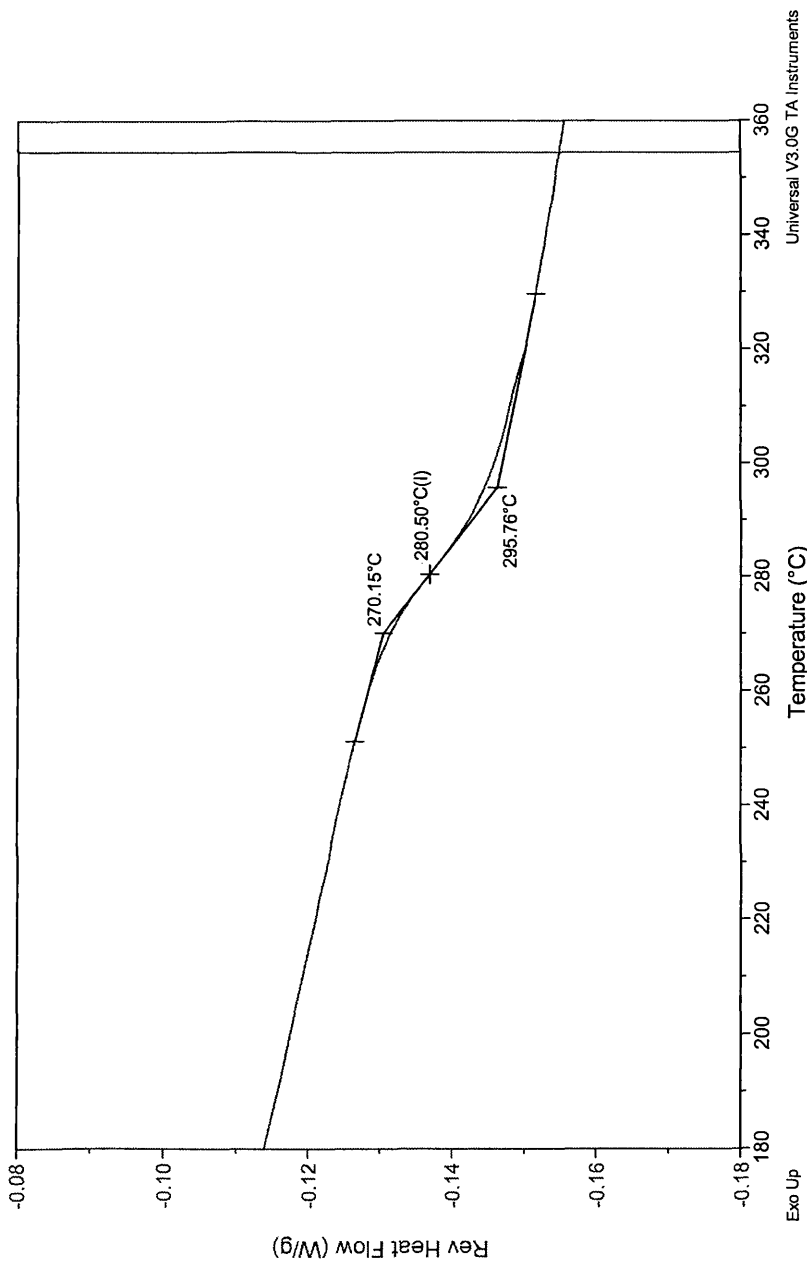
Figure App. 3.18: DSC of PMDABDA3

Figure App. 3.19: DSC of UDABDA1

DSC

File: C:\Sha Yang\UB2062204-031505.001
Operator: sha
Run Date: 15-Mar-05 11:11

223.77°C

233.45°C(I)

247.28°C

Rev Heat Flow (W/g)

Temperature (°C)

Exo Up

Universal V3.0G TA Instruments
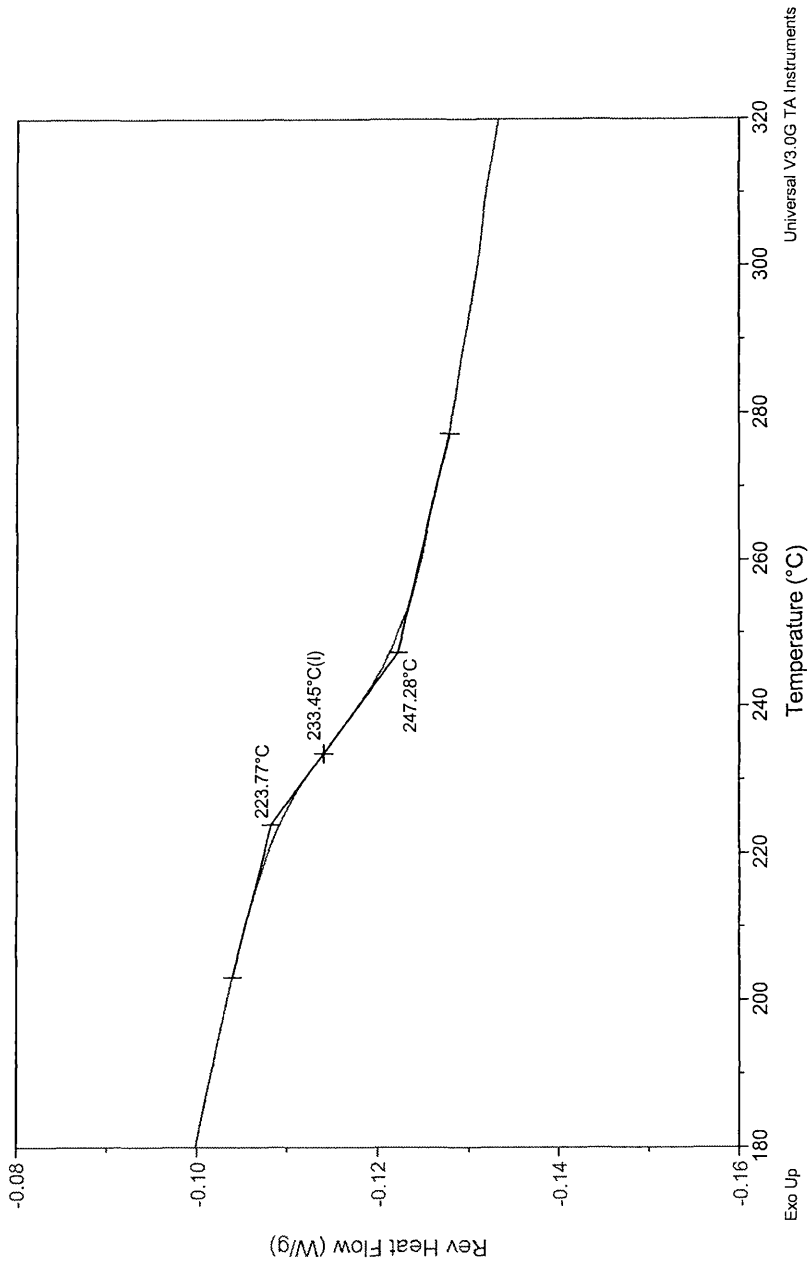
Figure App. 3.20: DSC of UDABDA2
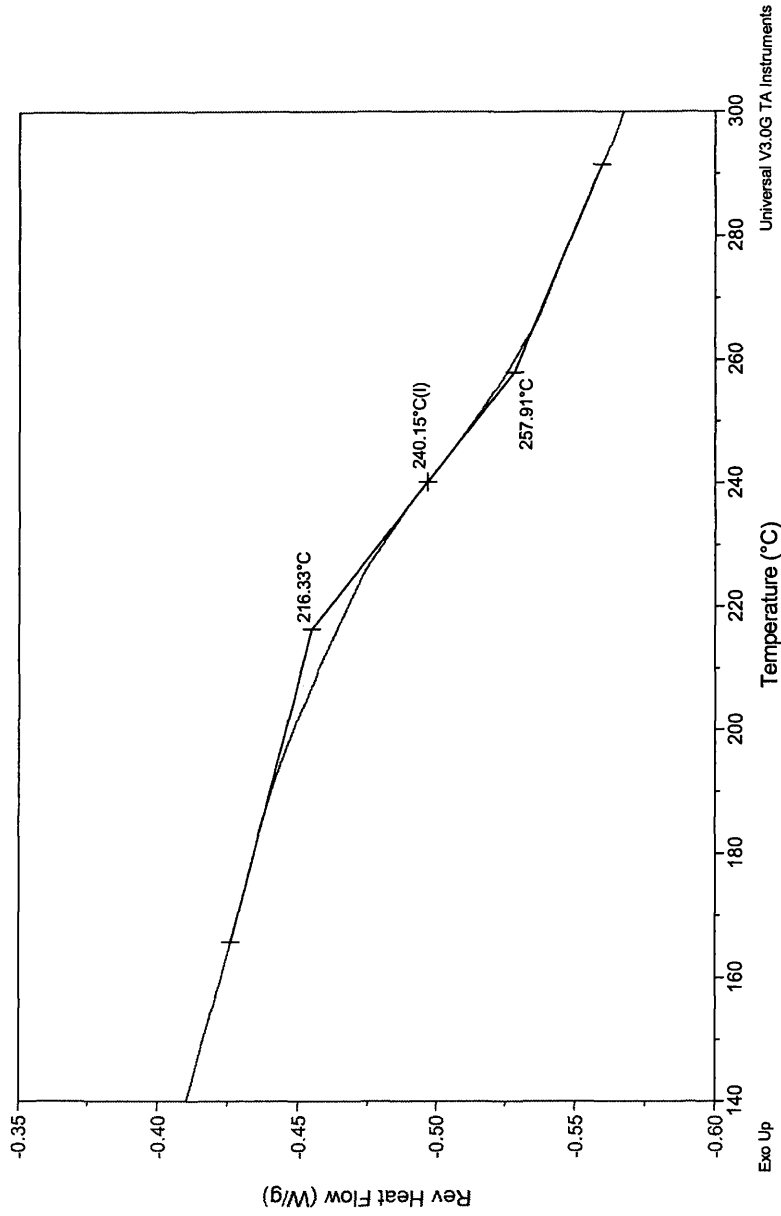
Figure App. 3.21: DSC of UDABDA3
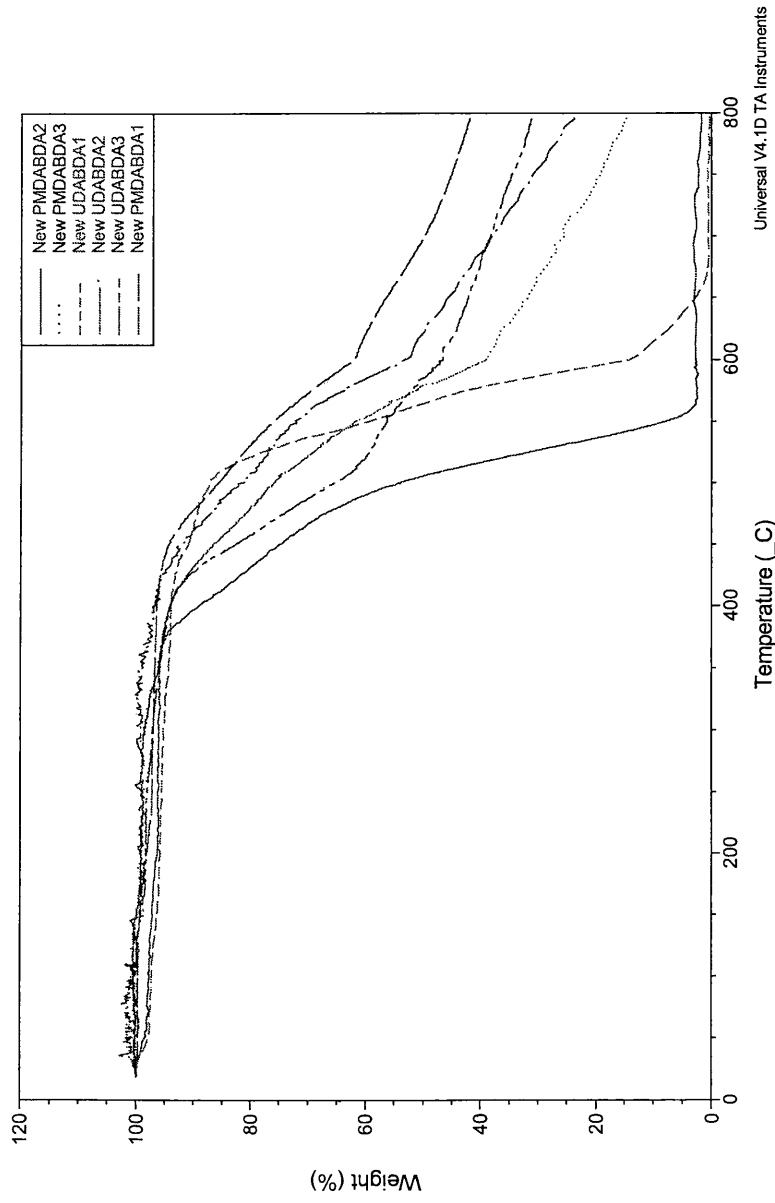
Figure App. 3.22: TGA of six polyimides
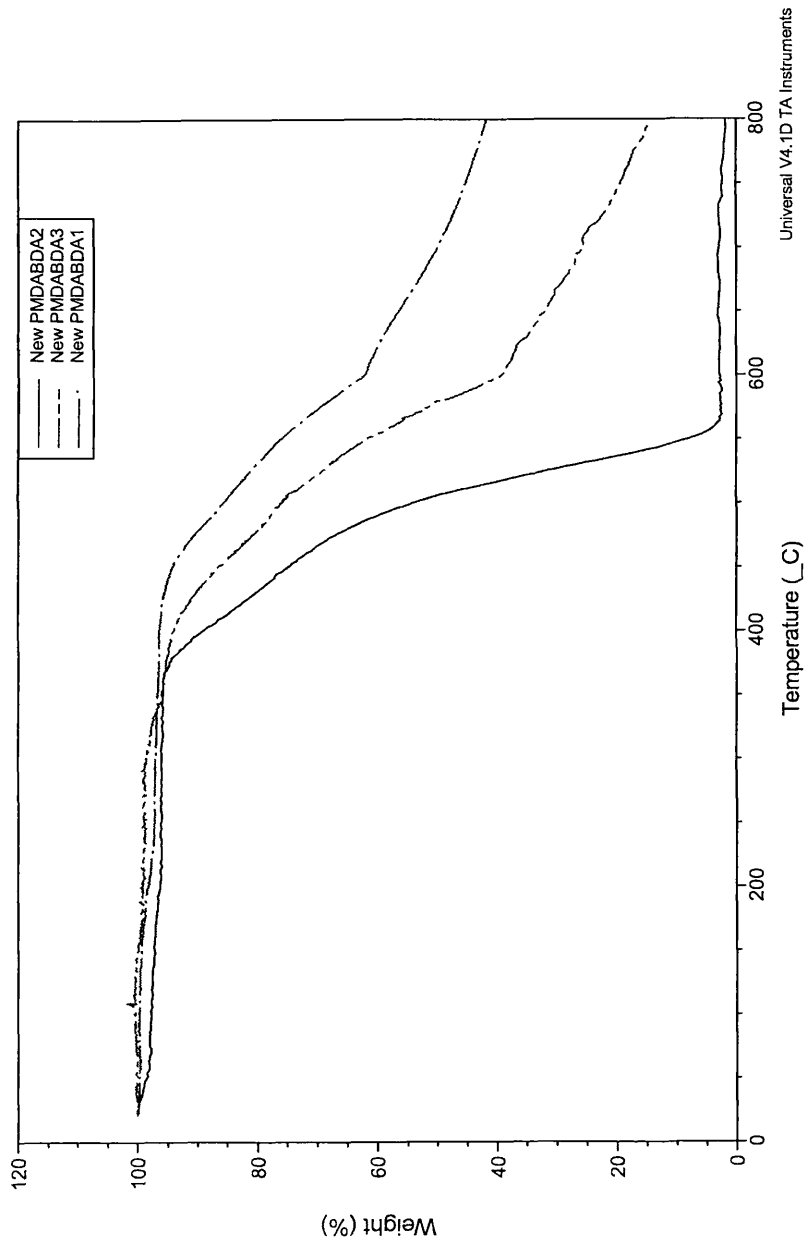
Figure App. 3.23: TGA of PMDA series
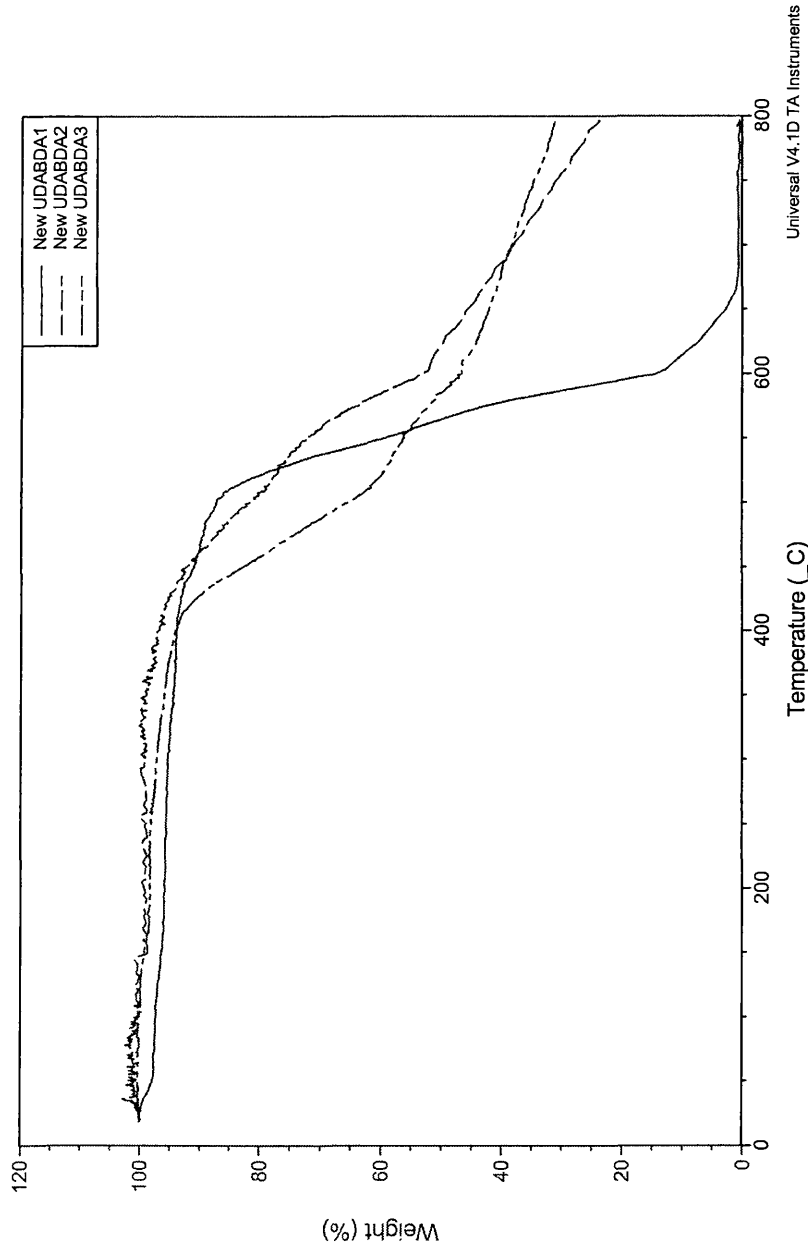
Figure App. 3.24: TGA of UDA series
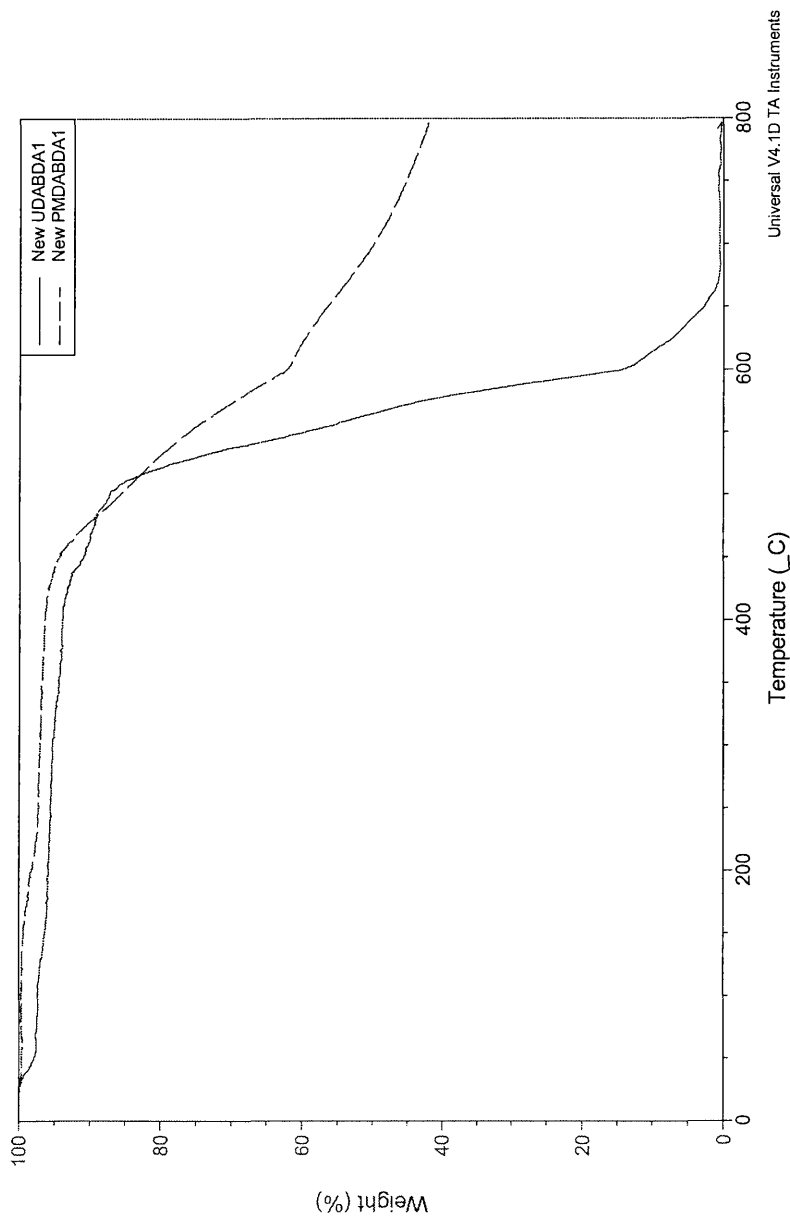
Figure App. 3.25: TGA of UDABDA1 and PMDABDA1
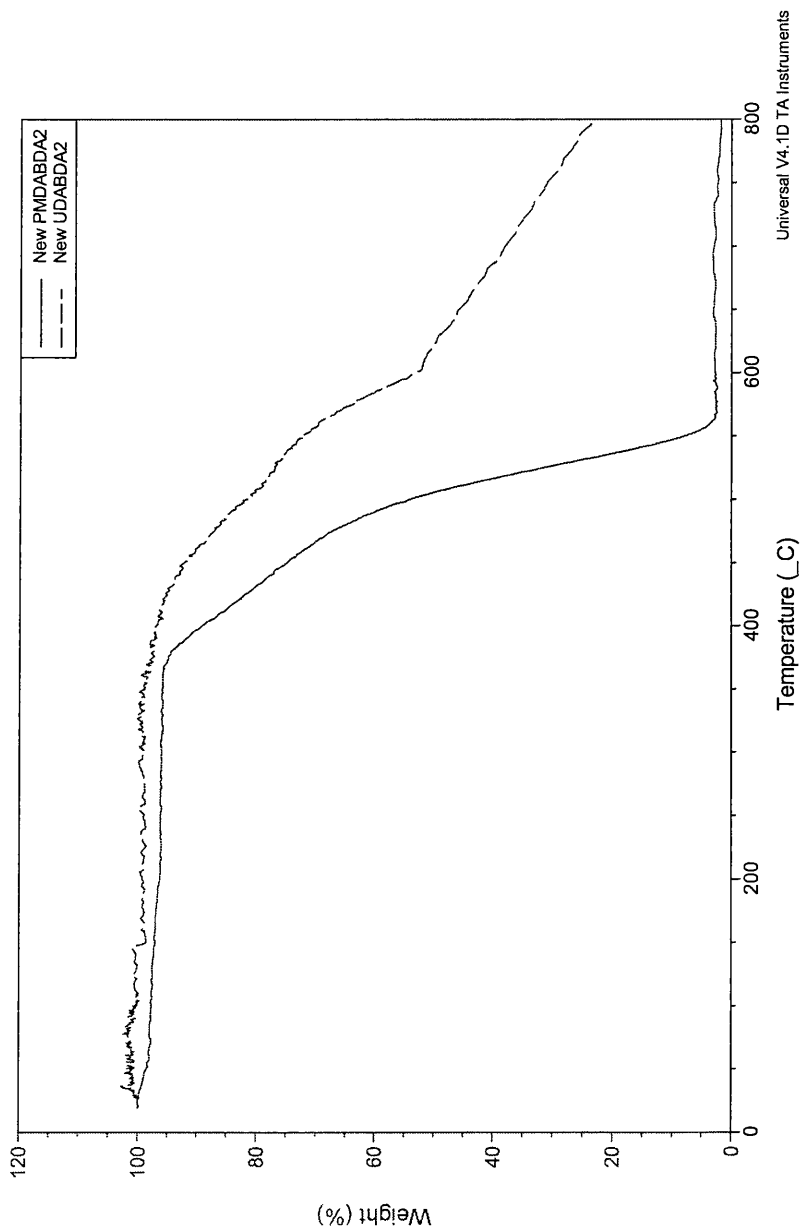
Figure App. 3.26: TGA of UDABDA2 and PMDABDA2
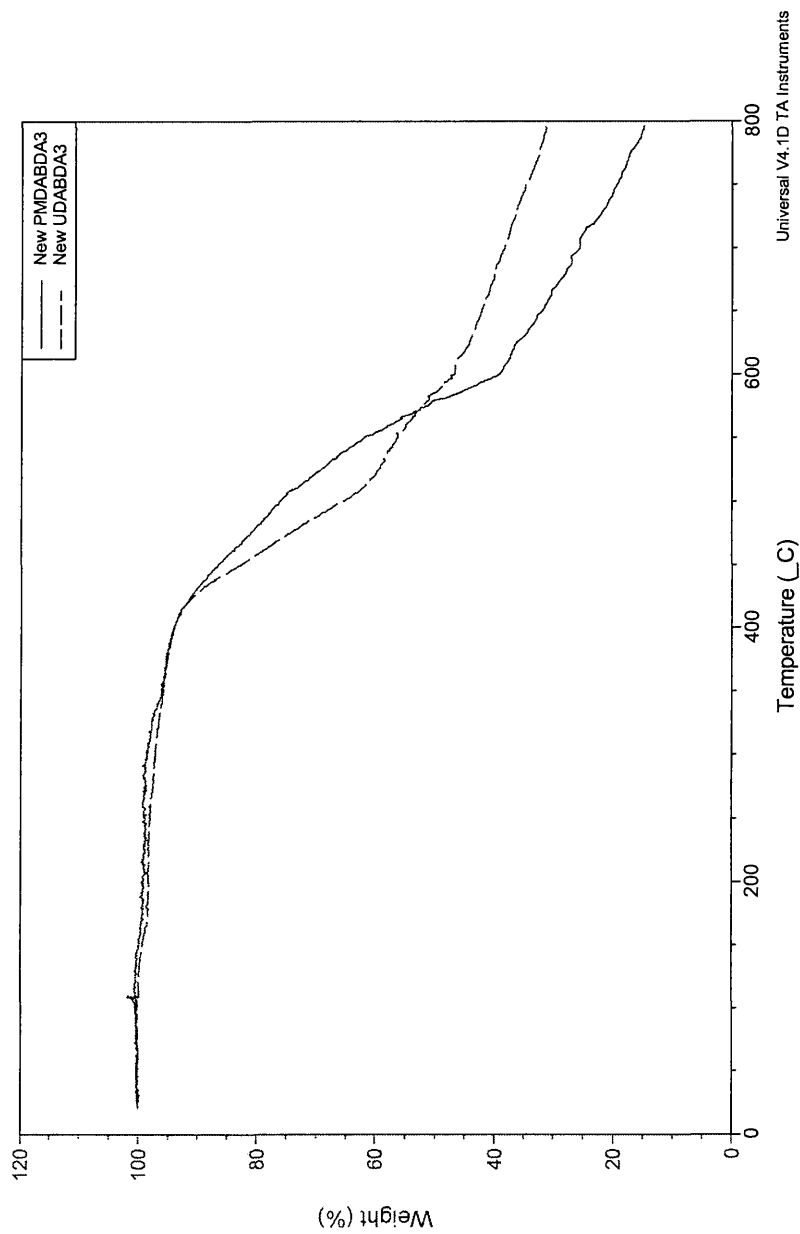
Figure App. 3.27: TGA of UDABDA3 and PMDABDA3
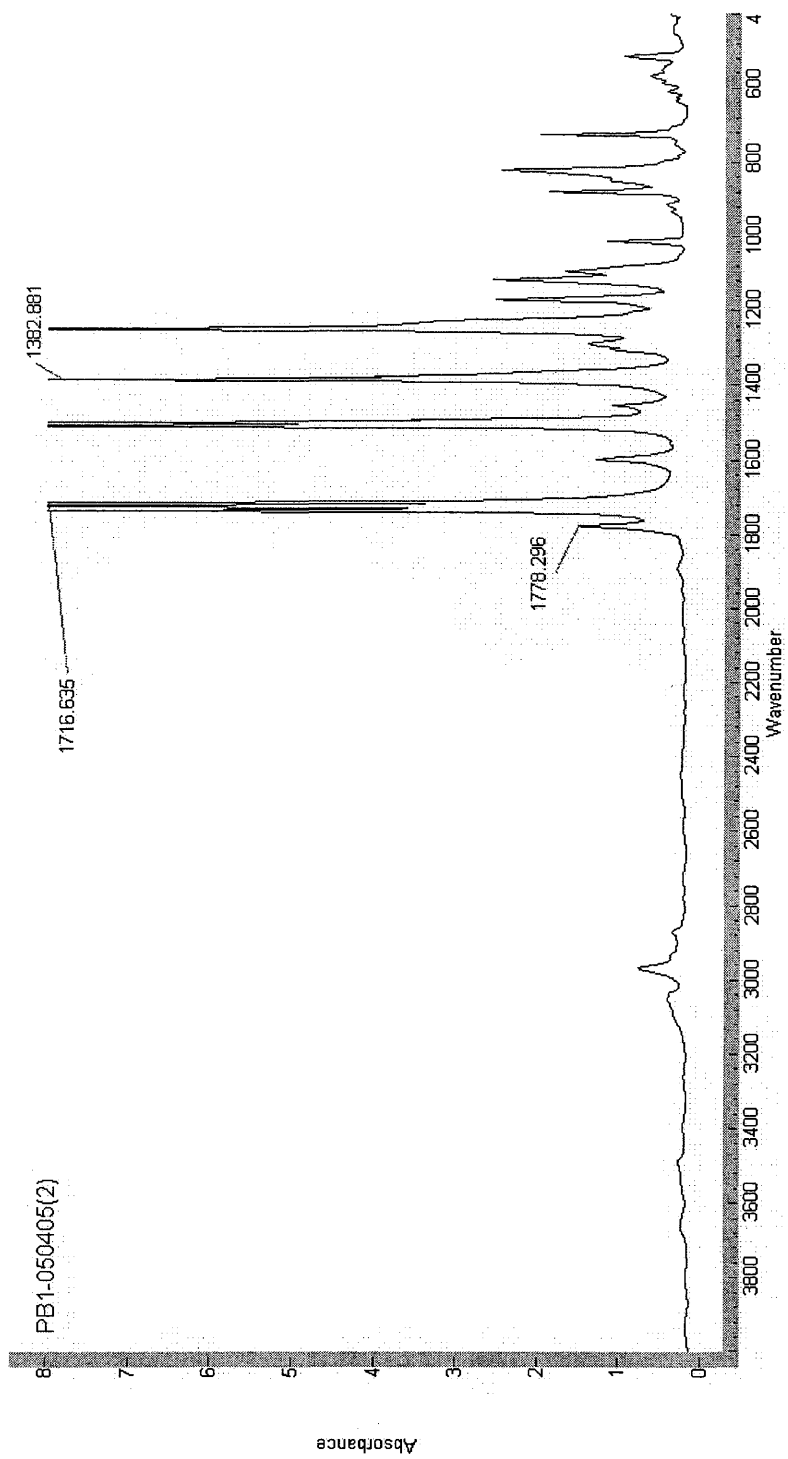
Figure App. 3.28: IR of PMDABDA1
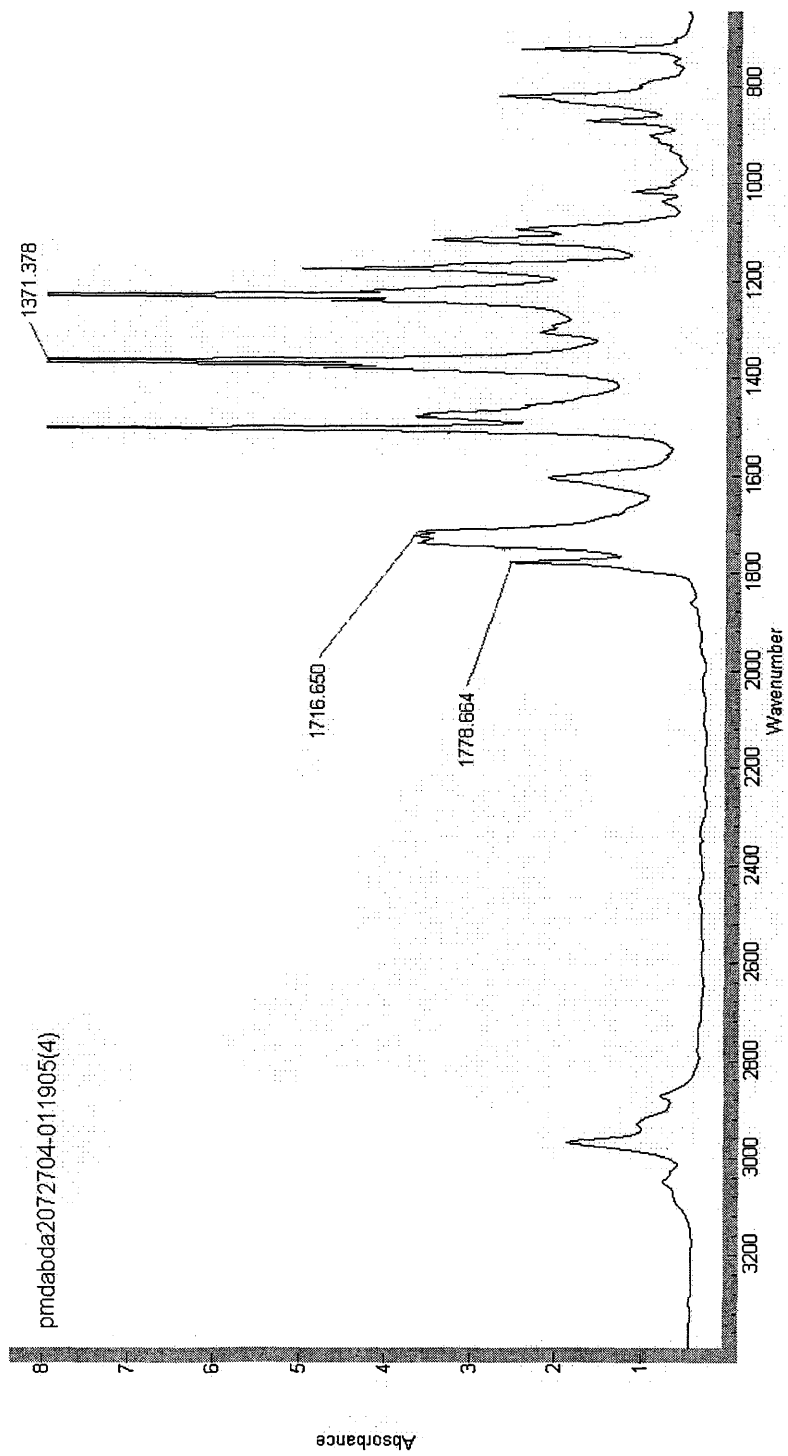
Figure App. 3.29: IR of PMDABDA2

Multi-Spectral Document2(1)
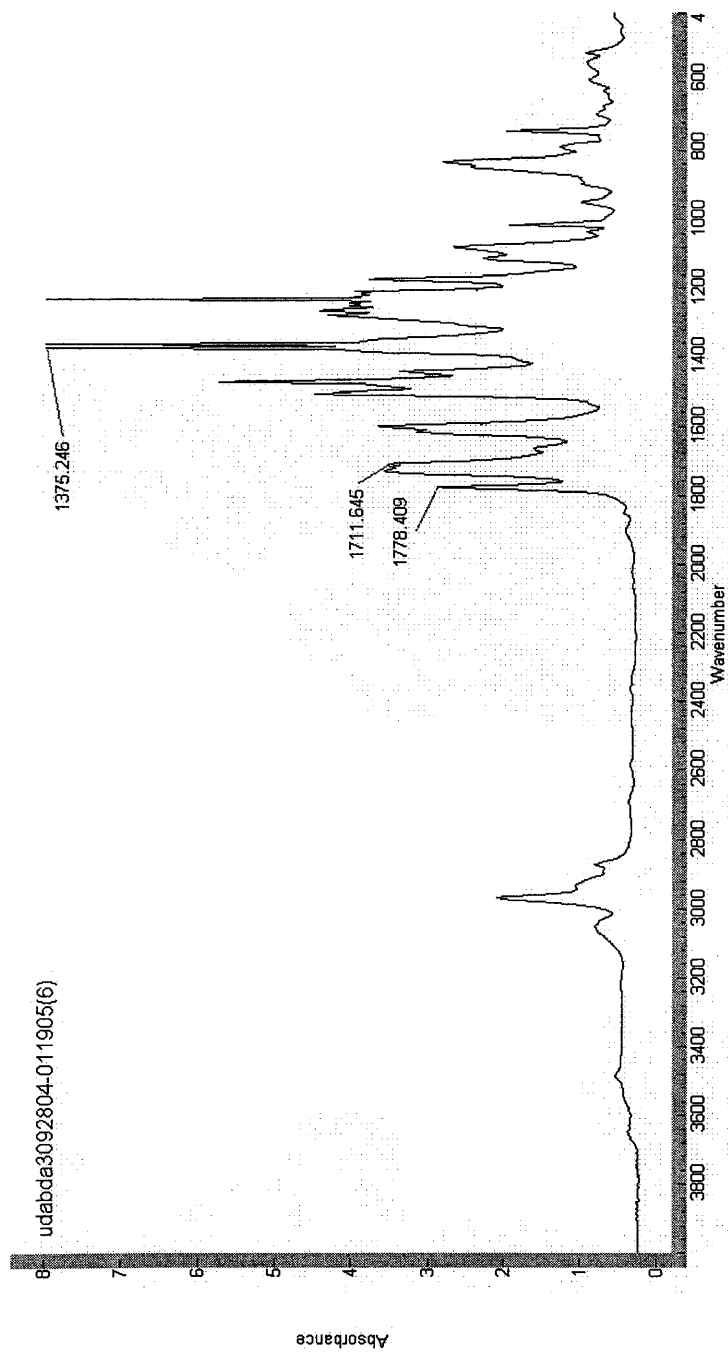
1734.966

1374.278

1779.175

Wavenumber

Absorbance
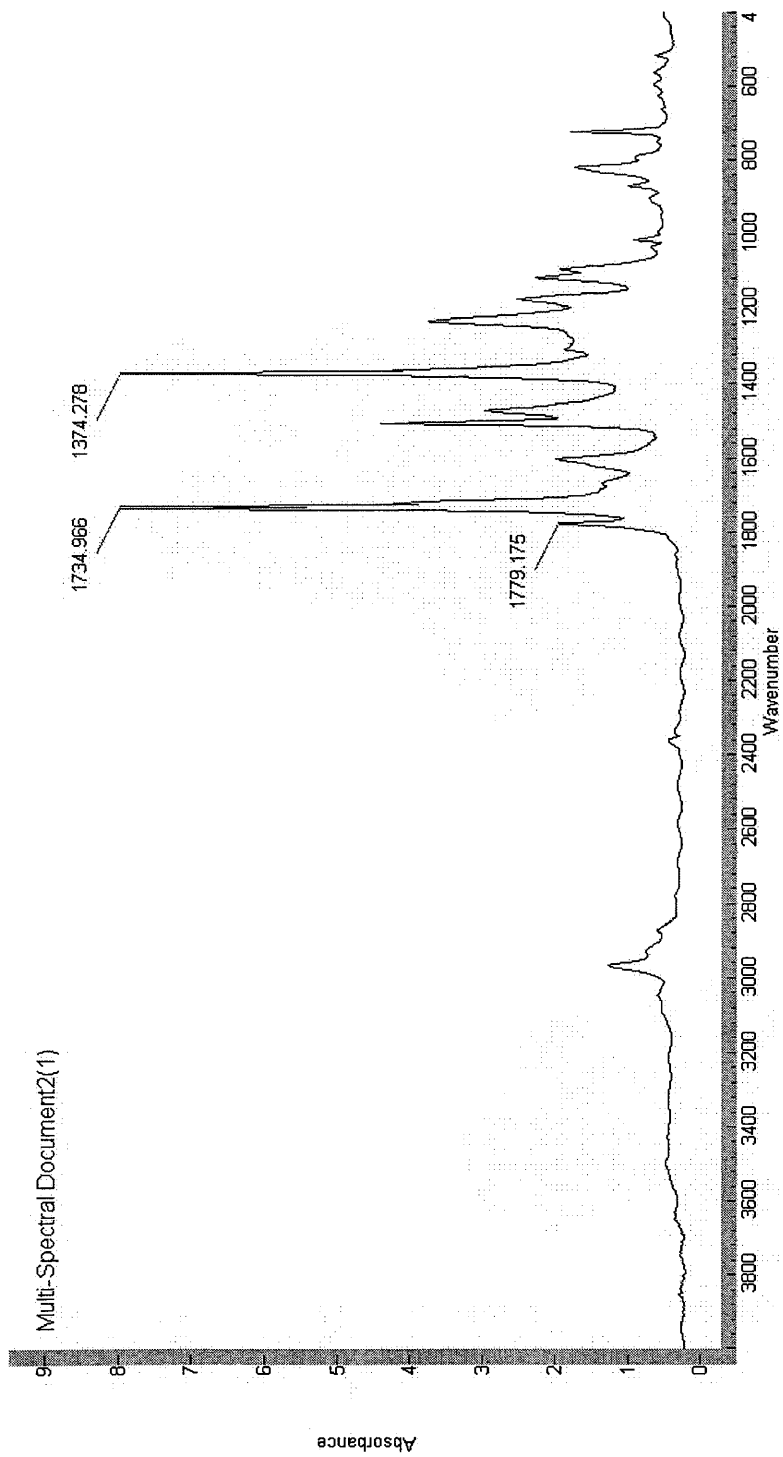
Figure App. 3.30: IR of PMDABDA3
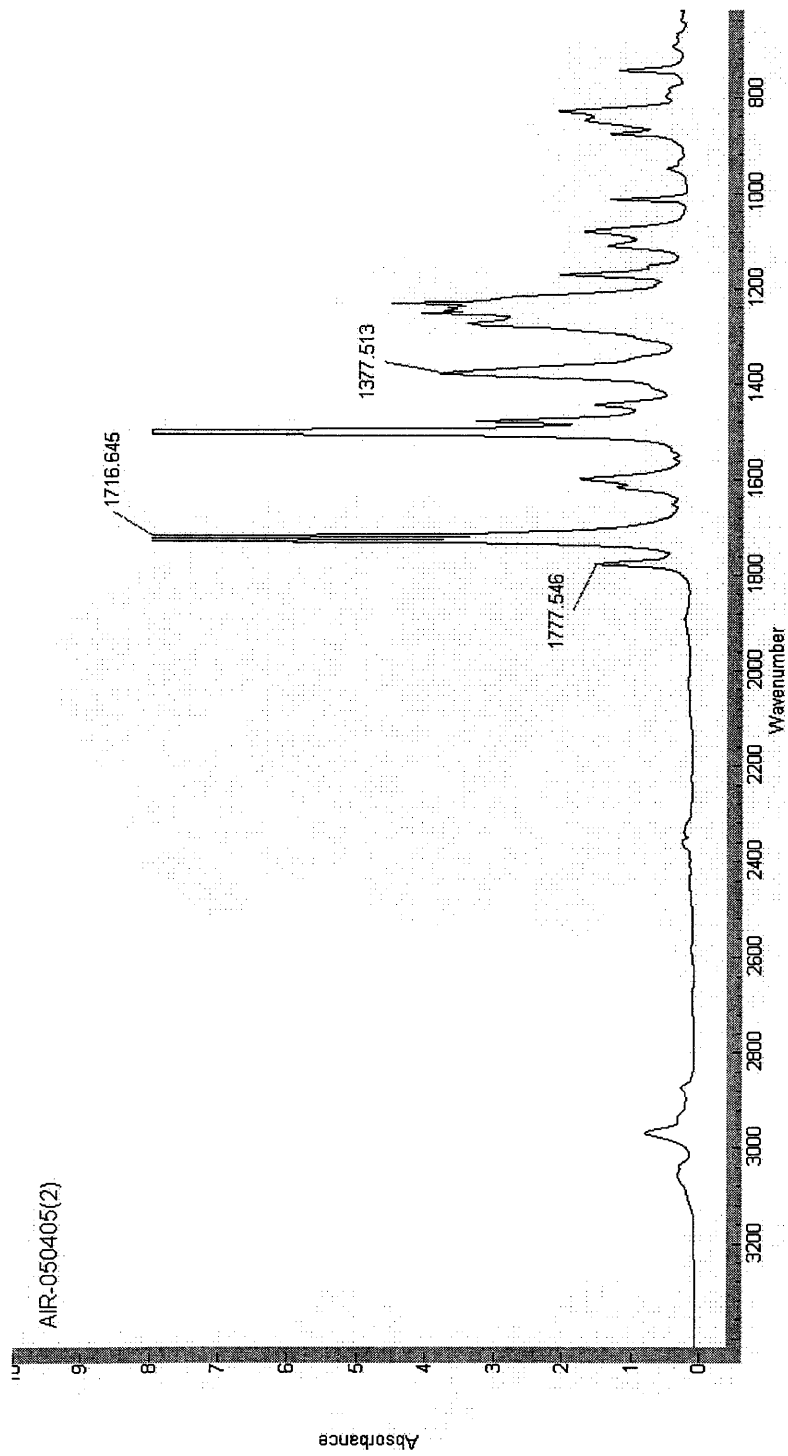
Figure App. 3.31: IR of UDABDA1
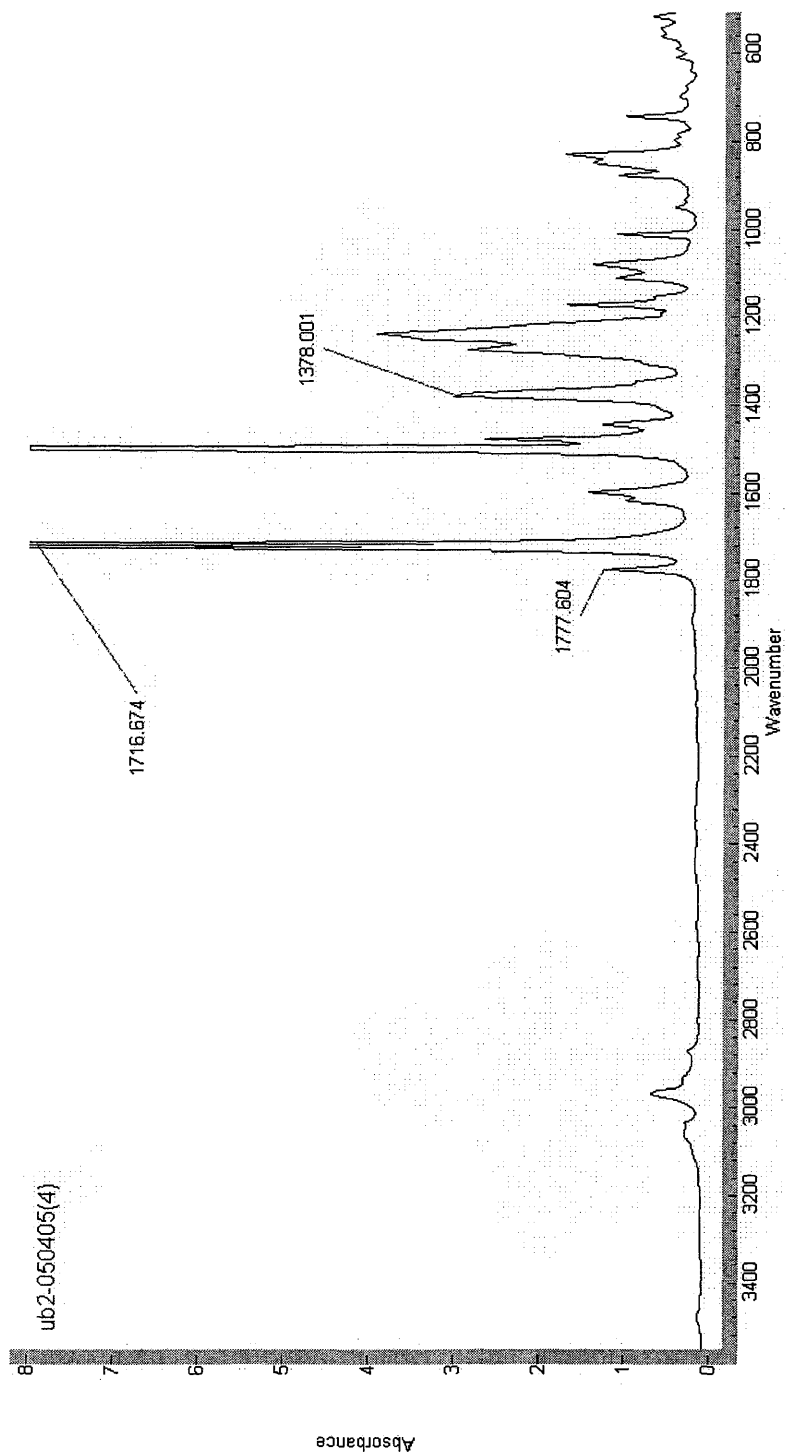
Figure App. 3.32: IR of UDABDA2

Figure App. 3.33: IR of UDABDA3
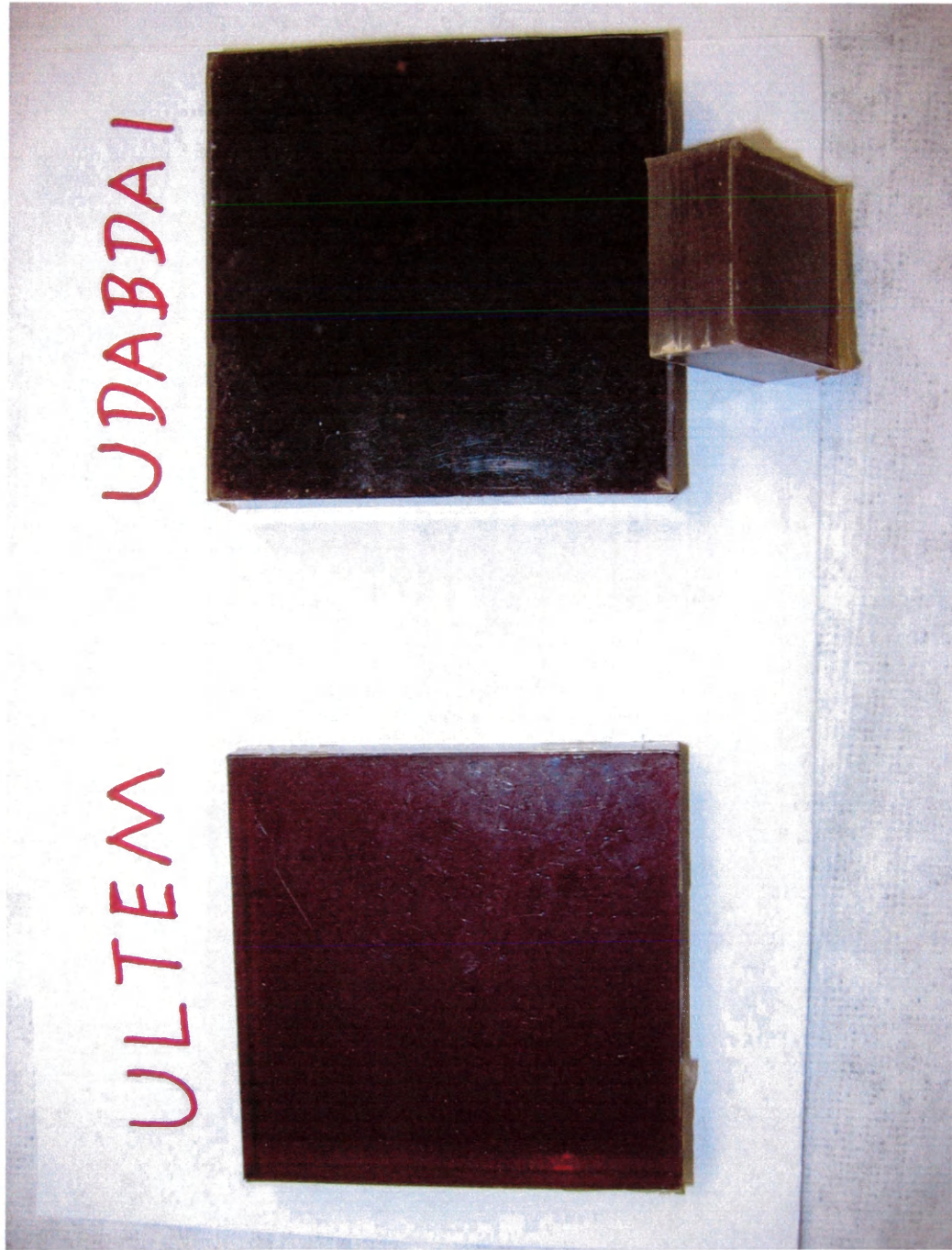
Figure App. 4.1: Blocks of ULTEM and UDABDA1
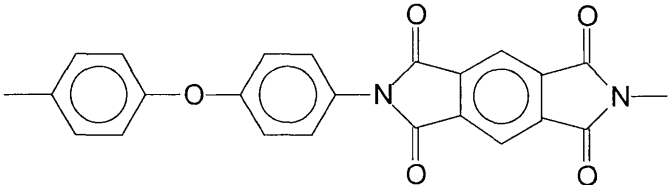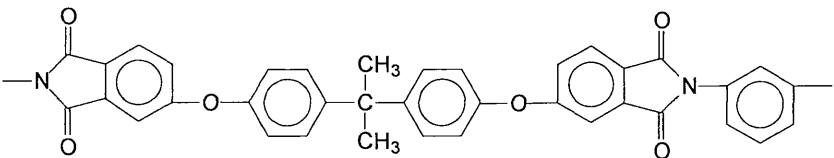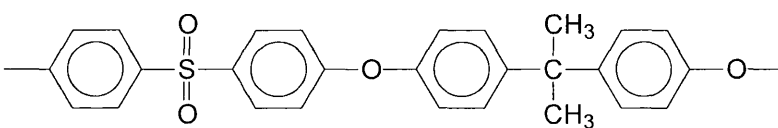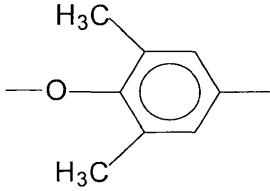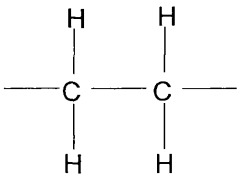
Table App. 4.1: Blocks* made for test as shields against high-energy cosmic radiation

	Dimension (inch)	Mass (g)	Moles of H per gram	Area density (g/cm^2)
Ultem	3x3x1.579O	290.6	0.041	5.005
polysulfone	3x3x1.6405	290.8	0.050	5.008
Noryl731	3x3x1.8071	275.7	0.0666	4.748
PMDABDA1	3x3x2.0938	290.5	0.0405	5.003
	3.5x3.5x0.2490[b]	39.2		0.495
PMDABDA2	Press one, not melt	/	0.0493	/
PMDABDA3	N/A	/	0.0548	/
UDABDA1	3x3x1.5905	282.8	0.0469	4.870
	3.5x3.5x0.1329	31.0		0.392
UDABDA2	3x3x1.7068	280.3	0.0526	4.827
UDABDA3	N/A	/	0.0561	/

*All the blocks were made in Langley NASA lab.

Table App. 4.2: Commercial polymers being considered. Kapton and polyethylene have been included for reference.

Name	Formula	Structure	Moles of H per gram
Kapton	$C_{22}H_{10}O_5N_2$		0.026
Ultem	$C_{37}H_{24}O_6N_2$		0.041
Udel	$C_{27}H_{22}O_4S$		0.050
PPO	C_8H_8O		0.067
Polyethy —lene	C_2H_4		0.143

VITA

<u>Sha Yang</u>

Sha Yang was born in Anhui, P. R. China, and November 17, 1980. He graduated from Dongfeng High School in July 1998. The author received his Bachelor of Science at University of Science and Technology of China in July 2003 with a degree in Chemistry.

In August 2003, the author became a graduate student for Master of Science studying in the Department of Chemistry at the College of William and Mary.

Upon graduation the author plans on attending Virginia Tech to pursue a Doctorate in Polymer Chemistry.